A Nuclear-Powered Trailing Suction Hopper Dredger

Researching the transient load capabilities

Msc Marine Technology

F.N.L. Aberson Bodewes

Delft University of Technology

TU Delft

A Nuclear-Powered Trailing Suction Hopper Dredger

Researching the transient load capabilities

by

F.N.L. Aberson Bodewes

to obtain the degree of Master of Science
at the Delft University of Technology,

Student number:	4591984	
Report number:	MT.24/25.004M	
Project duration:	November, 2023 - September, 2024	
Thesis committee:	Prof. dr. ir. H. Polinder,	TU Delft, supervisor
	Prof. dr. ir. B.J. Boersma	TU Delft
	Ir. K. Visser	TU Delft
	Ir. M. Kom	Boskalis
	Ir. C.F.M. Van den Berg	Boskalis
Faculty:	Faculty of Mechanical engineering	TU Delft

Cover: New 31.000 m3 TSHD currently being built for Boskalis

An electronic version of this thesis is available at http://repository.tudelft.nl/.

TU Delft

Boskalis

Preface

This report presents my final thesis for the Master 'Marine Technology' at Delft University of Technology. My thesis research should contribute to establishing the technical feasibility of powering a large dredging vessel by an on-board nuclear reactor in the future.

Throughout my thesis research, I had the privilege of working as an intern at Boskalis, a leading global dredging-, offshore contractor- and maritime services- provider. It is valuable to gain experience in such company and to get reminded of the practical side of research. I thank the R&D- and CFS departments at Boskalis for allowing me to research such a niche topic with them. More importantly, I would like to thank Martijn Kom and Chris van den Berg for both their support in tackling the hurdles associated with this topic and their availability at all times. Next, I extend my sincere thanks to my supervising professor at TU Delft, Prof. dr. ir. H. Polinder, for the feedback on my work and the help in steering through a thesis project.

In parallel, this report marks the end of my studies in Delft. From a young age, I have always been fascinated by the maritime industry. Pursuing a BSc and a MSc in Marine Technology was the perfect fit at the time, and remains a decision I am grateful for today and tomorrow. Throughout the program, I gained both knowledge and interest in topics such as: alternative fuels- and emission-reduction methods for the maritime fleet. The topic of nuclear-powered merchant shipping - and the associated zero-emission potential - gained significant momentum in these past 2 years of my studies. This triggered me to take part in something that could be the next step in revolutionising the Maritime industry.

Finally, a big thanks to my family, friends and girlfriend for their unconditional support and motivation throughout the course of this project.

F.N.L. Aberson Bodewes
Delft, September 2024

Summary

Today's necessity- and goal to reduce carbon emissions in tandem with finite fossil resources and rising oil prices, demand for an alternative and cleaner energy source to power the world dredging fleet. In parallel, recent research in naval architecture iterates the potential role for nuclear-based propulsion on board of 'energy-intense' merchant vessels (approx. 20 MWe+ installed power) [16][20][23]. Powering a (large) trailing suction hopper dredger (30.000m3+) by an on-board small modular nuclear reactor would cut direct greenhouse gas emissions by 100%.

The power demand on board of trailing suction hopper dredger is fluctuating continuously. A reactor is typically applied for supplying constant power. The objective of this thesis was to research the transient load capabilities of a nuclear-powered trailing suction hopper dredger.

First, for the on-board nuclear installation, a graphite-moderated high temperature gas reactor was opted for which is cooled by helium gas. This reactor type has a technology readiness level of 9 and small-modular-reactor concepts of this type are being developed. Both the open- and closed helium Brayton cycle concepts show greatest potential for power conversion. It was shown that the reactor, the heat exchangers and the turbomachinery play an important role in both the overall efficiency of operation and the transient load limits of the system as a whole.

Second, a thermodynamic model was built to be able to simulate the effects of different control mechanisms in realising load-following. Bypass- and compressor throttling control performed best and allowed the reactor to ramp down at lower rate, which is a favourable feature. For a 100% reduction in power output, the reactor would have to ramp down to 47% and 34% of nominal power respectively.

Third, it was investigated how the limitations in load-following would effect the operational profile of a HTGR-powered TSHD. The suggested closed helium Brayton cycle cannot perform adequate load following to the fluctuating demand of a conventional TSHD today without an auxiliary source of energy. When keeping reactor ramping rates below 10%/minute, a 25MWe HTGR-powered TSHD would see peaks in power imbalance up to 10 MW. However, a 3MWh ESS was considered to perform power-take-in and power-take-off. In presence of such auxiliary power source, the operational profile of a TSHD would not have to be changed.

Looking ahead, it is crucial to investigate the impact of repetitive power transients on the controllability- and lifespan of both the reactor and other components within the power cycle. Additionally, a more in-depth study of the aerodynamic characteristics of the helium turbomachinery is necessary. Lastly, incorporating supplementary nuclear kinetics analysis could help validate the findings presented in this report.

Keywords: Gen-IV, SMR, Modular high-temperature gas-cooled reactor, HTGR, Control mechanisms, Load following, Intercooled, Recuperated, Valve, Bypass, Inventory, Throttling, Thermodynamic modelling, Brayton cycle, Closed cycle, Direct cycle, TSHD, Nuclear ship

Contents

List of Figures

List of Tables

Nomenclature

Abbreviations

Abbreviation	Definition
BC	Bypass Control
CAPEX	Capital Expense
CHX	Cooling Heat Exchanger
CO2	Carbon Dioxide
CSC	Compressor Speed Control
CTC	Compressor Throttle Control
ESS	Energy Storage System
HCHE	Helical Coil Heat Exchanger
HPC	High Pressure Compressor
HTGR	High-temperature Gas-cooled reactor
IHX	Intermediate Heat Exchanger
IMO	International Maritime Organisation
INVC	Inventory Control
ISA	International Standard Atmosphere
LPC	Low Pressure Compressor
LMTD	Logarithmic Mean Temperature Difference
MGO	Marine Gasoil
MSR	Molten Salt Reactor
NOx	Nitrogen oxides
NTU	Number of Transfer Units
OPEX	Operating Expense
PBR	Pebble Bed Reactor
PCHE	Printed Circuit Heat Exchanger
PFHE	Plate (&fin) Heat Exchanger
PWR	Pressurised Water Reactor
REC	Recuperator
RPM	Revolutions Per Minute
SMR	Small Modular Reactor
STHE	Shell and tube
SOx	Sulfur Oxide
TRISO	TRistructural-ISOtropic
TRL	Technology Readiness Level
TSHD	Trailing suction hopper dredger
TTC	Turbine Throttle Control
(v)HTR	(very) High Temperature Reactor
(v)SMR	(very) Small Modular reactor

Symbols

Symbol	Definition	Unit
A	Heat transfer area	[m^2]
C_p	Specific heat at constant pressure	[J/(kg·K)]
h	Heat transfer coefficient	[W/(m^2·K)]
k_w	Thermal conductivity of the wall material	[W/(m·K)]
m	Mass	[kg]
$\dot{m}$	Mass flow rate	[kg/s]
P	Pressure	[Pa]
R	Thermal resistance	[K/W]
$\dot{Q}$	Heat transfer rate	[W]
T	Temperature	[K]
Δh	Enthalpy change	[J/kg]
ΔT	Temperature difference	[K]
U	Overall heat transfer coefficient	[W/(m^2·K)]
V	Velocity	[m/s]
δ_w	Wall thickness	[m]
ϵ	Effectiveness	dimensionless
Φ	Energy balance term	Depends on context
ρ	Density	[kg/m^3]

1

Introduction

1.1. Background

Since 1960 trailing suction hopper dredger vessels (TSHD) have been key assets in accommodating the growing demand for dredging around the world. A TSHD is an oceangoing vessel that collects sand, clay and silt from the seabed and transports it to other areas. Today, the vast majority of these vessels are powered by burning fossil fuels in an internal combustion engine.

In 2022, the international shipping accounted for nearly 3% of the world's greenhouse gas emissions. In July 2023, the International Maritime Organisation set a goal of net zero emissions from ships "by or around, i.e. close to 2050". In addition to the IMO trajectory, the European Union has implemented several regulations to address emissions from shipping within its jurisdiction. Besides the regulatory pressure, companies set goals to decarbonise their products and/or services - such as Boskalis. Boskalis operates and owns dredging vessels that consume significant energy during operation. Carbon emissions of these dredging operations are to be reduced.

Today's necessity to reduce carbon emissions in tandem with finite fossil resources and rising oil prices, demand for an alternative and cleaner energy source to power the world dredging fleet.

A Small modular reactor (SMR) is the overarching term for any advanced small nuclear fission reactor up to 300 MWe per module. A SMR emits zero direct greenhouse gas emissions and the carbon dioxide equivalent per kilowatt-hour is estimated at 5 gram only, versus 738 gram for conventional MGO-based power generation [18]. Thus, when it would be possible to power a dredging vessel by an on-board SMR, this would cut direct greenhouse gas emissions by 100% and the carbon-equivalent per kWh by 99%.

1.2. Motivation

Today over 160 vessels have a nuclear-based propulsion on board. However, little is known about these ships as these are all navy class or sailing under governmental exceptions. These ships - except one- are powered by a pressurised water reactor. The past 70 years proved that there was no benefit to sail commercial ships on a pressurised water reactor (PWR). Only four nuclear-powered merchant ships have been built so far, all of them government-led projects begun mostly for development- and testing reasons rather than purely commercial ones. Common challenges are: high cost, safety concerns, public perception and regulatory barriers [38].

The latest generation reactor technologies - in succession of the PWR - is called Gen-IV. A small modular reactor is Gen-IV. Advancements in small-modular-reactor technology has lead to better safety, a lower proliferation risk, higher burn-up and better dynamic load properties of these reactors [1]. Recent research states that the molten salt reactor (MSR) and the high temperature gas reactor (HTGR) are expected to have greatest potential for marine application in the future [16] [20] [23]. The HTGR has a higher technology-readiness-level (TRL) - up to 9 in China - compared to the MSR with a TRL of 3

[14][35]. Based on the aforementioned arguments, there is both momentum and interest to study the potential of an on-board HTGR.

In parallel, recent research in naval architecture iterates the potential role for nuclear-based propulsion on board of 'energy-intense' vessels (approx. 20 MWe+ installed power) [16][20][23]. It mentions the potential for significant power at lower OPEX and independence for refuelling. A large TSHD (30.000 m3+) is a type of dredging vessel with an installed power capacity of more than 25 MWe. A nuclear-powered TSHD would not directly exhaust any harmful gasses such as SOx, NOx or CO2.

Therefore, today's rapid developments in small-modular-reactor concepts, the prevailing advantages, in combination with the necessity- and will to decarbonise, demonstrate both the social and scientific benefit of exploring the potential of a nuclear-powered TSHD.

1.3. Problem definition

Much research is required to establish technical feasibility of powering a TSHD by an on-board HTGR. In addition to the fact that commercial-nuclear-powered shipping is in its infancy itself, a TSHD is in many aspects different than a regular vessel too. A contribution to establishing technical feasibility of powering a TSHD by an on-board HTGR is required.

The mission of a TSHD is unique and may change anytime. The vessel requires much power for its dredging operations and the power demand may fluctuate quickly. The heat produced by fission inside the HTGR is to be converted into (electrical) power. There are different concepts to convert this energy and each concept will have its own characteristics. It is unclear which power conversion concept to choose on board of a TSHD and how this would impact the performance of the vessel. In addition to the limits in dynamic power output for a HTGR, the power plant behind it may have limits as well. This would have an influence on the transient load capability of the TSHD.

As these aspects have not been studied before, this limits our understanding of the technical feasibility of powering a TSHD by an on-board HTGR in the future. Hence, this limits our understanding of the role that on-board nuclear power could fulfil in bringing carbon emissions down to zero.

1.4. Research objective

The main objective of this study is to contribute to establishing the technical feasibility of powering a TSHD by an on-board high-temperature gas reactor in the future. More specifically: researching the transient load capabilities of such nuclear-powered TSHD concept.

1.5. Research questions

The main research question is: **Could the transient load capabilities of a nuclear-powered TSHD match the dynamic operational power profile of a TSHD?**

To answer the main research question, the question is split into multiple sub-questions. The first sub-questions are covered by a literature study:

1. Why a nuclear-powered TSHD?
2. Which GEN-IV reactor technology to install on board of a future nuclear-powered TSHD?
3. How to convert the heat from the reactor into (electrical) power?
4. How to control a varying power demand?
5. What would a first iteration power train look like?

Resulting from a a gap analysis, the successive sub-questions below form the core of this research.

6. How do the different sub-systems in the closed helium Brayton cycle influence the overall load-following performance of the power cycle?
7. What is the effect of the different power control mechanisms on the load following capability of the closed helium Brayton power cycle[1]?
8. How would the load-following characteristic of the suggested HTGR power cycle effect the operational profile of a TSHD?

1.6. Methodology

The first part of this research is done via literature research. The second part of this research will first assess the role of different sub-systems in the overall power cycle. Hereafter, it is attempted to simulate both the thermodynamic- and aerodynamic characteristic of the suggested power cycle via a model. Subsequently, the model is used to run different scenario's. The results from simulating the suggested system characteristics in combination with varying power demand profiles, should help answer the sub-questions in the second part. Simulations are modelled in Matlab Simulink software.

1.7. Structure of the report

- Chapter 2 - 'Literature study' covers sub question 1 to 5.
- Chapter 3- 'System characteristics of an on-board HTGR' covers sub question 6.
- Chapter 4 - 'Model Description' provides background and detailed information about the model configured in the duration of this study.
- Chapter 5 - 'The effect of different power control mechanisms' should answer sub-question 7
- Chapter 6 - 'Effect load following characteristic HTGR power cycle on powering a TSHD' covers sub question 8.
- Chapter 7 - 'Conclusion' contains the conclusion and recommendations.

[1] The 'Brayton power cycle' will be introduced in the literature study in chapter 2

2

Literature study

This chapter contains a literature study. The literature study provides answers to the first research sub-questions. In addition, this chapter helps the reader understand the second part of this research, which forms the core of this research.

2.1. A nuclear-powered trailing suction hopper dredger

This section answers the sub-question: Why a nuclear-powered trailing suction hopper dredger?

In recent years, momentum and interest around the potential for nuclear-powered merchant shipping has increased. But why a nuclear-powered trailing suction hopper dredger? There are different arguments to explore the potential of a nuclear-powered TSHD. Three main arguments are discussed in this section.

Potential to cut emissions
Although the total emissions of the worldwide dredging fleet is ca. 0.6% of the total CO2 emissions of global shipping, large dredging vessels - like a large TSHD - emit significant carbon emissions per ship. A SMR emits zero direct greenhouse gas emissions and the carbon dioxide equivalent per kilowatt-hour is estimated at 5 gram only, versus 738 gram for conventional MGO-based power generation [18]. Thus, when it would be possible to power a TSHD by an on-board SMR, this could potentially cut direct greenhouse gas emissions by 100% and the carbon-equivalent per kWh by 99%.

High energy consumption loans
Undoubtedly, a nuclear-powered TSHD vessel will require very high initial capital expenditure. However, for large energy consuming vessels the operational expenditure could potentially be smaller [16]. Today, dredging companies pay millions of dollars per year per vessel in bunker expenses, which fluctuate greatly as well due to instability in oil prices. In addition, it is expected that finite fossil resources and levies on carbon emissions will only increase these operational costs in the (near) future [10]. In accordance with the aforementioned, the concept of on-board nuclear power will be most viable for vessels with high energy consumption, like a large energy-intense TSHD. Lower OPEX could offset the CAPEX. Previous studies talk about a potential 'economical break-even' sweet spot from 20 MWe+ when assessing the lifetime cost - assuming favourable circumstances [20] [23][16].

Independence for refuelling
Nuclear power would allow for longer refuelling periods and therefore a stronger independence for refuelling. Technically, it would be possible not having to refuel ever again given the energy density of a kg of 5% enriched uranium* being $2 * 10^6$ times higher compared to a kg of MGO. However, it is expected that regulation will likely not allow commercial ships to keep unlimited nuclear fuel on board and therefore a period of 5 years is more realistic - in line with mandatory dry dock [28]. Not having to bunker allows for continuous operation which could be very favourable- especially when operating in remote areas. Finally, given the independence for refuelling in accordance with the relative lower energy cost, operators could opt for using much more power. Increased power availability could enable

higher sailing speeds and larger dredging pumps, increasing daily production $(m^3)/day$ even further at potentially lower cost in terms of OPEX/work $(\$/m^3)$.

2.2. Gen-IV reactor technology

This section answers the sub-question: Which Gen-IV reactor technology to install on board of a future nuclear-powered trailing suction hopper dredger?

2.2.1. Current state nuclear-powered ships

More than 700 nuclear-powered vessels have been built in the past 70 years and over 160 nuclear-powered vessels sail around today. Unfortunately, little is known about these ships as these are all navy class or sailing under governmental exceptions. Currently, each vessel- except one- is powered by a Gen-III pressurised water reactor (PWR). The past 70 years proved that there was no benefit to sail commercial ships on a pressurised water reactor. Only four nuclear-powered merchant ships were constructed and operated. All four were government-led projects, begun mostly for developmental and testing reasons rather than purely commercial ones. The strongest hurdles showed to be: high cost, safety concerns, public perception and regulatory barriers [38].

In recent years, momentum around the potential for merchant nuclear-powered shipping lifted off again. The zero-emission potential, high- and volatile oil prices and a new generation of SMR's are key reasons for regained interest.

2.2.2. Developments in small modular reactors

A small modular reactor (SMR) is defined as a nuclear reactor of 300 MWe or less, designed with modular technology using module factory fabrication, pursuing economies of series production and short construction times [32]. A very Small Modular Reactor (vSMR) is defined as a nuclear reactor of 25 MWe or less. Today, generation IV reactors are defined as the next generation of nuclear reactors.

Following a literature study, it was concluded that the Molten Salt Reactor (MSR) and the (very) High Temperature Gas Reactor (HTGR) both have potential to be the Gen-IV reactor technology on board of a future marine vessel. The HTGR-technology has a higher technology-readiness-level (TRL) - up to 9 in China - compared to the MSR with a TRL of 3 [14][35]. Given the higher TRL, the HTGR will be the reactor technology discussed in this report.

2.2.3. Developments in high temperature gas reactors

The (v)HTGR is a graphite-moderated (very) high temperature gas-cooled reactors designed to operate with a high outlet temperature. The (V)HTGR is the modern version of the HTGR, featuring the same concept with higher outlet temperature. For sake of simplicity, the term HTGR will refer to either type in this report. The cooling medium through the reactor core is typically Helium. Helium gas has great characteristics being: chemically inert, non-flammable, in steady gaseous state between -260 to 1000+ degrees Celsius and superior heat transport ($Cp = 5.19J/gK$).

HTGR's are inherently safe because the fuel pellets have a negative temperature coefficient meaning that the rate of nuclear reactions goes down with a rising temperature. Thus, in the event of a loss of coolant accident, the rising temperature automatically slows down the fission rate. The reactor becomes quite hot but suffers no damage [1]. This is a game-changer considering the pressurised water reactors on board nuclear-powered vessels sailing today where a loss of coolant accident would be fatal in case no active safety measures are undertaken.

Today, different HTGR concepts are being developed all over the world. Figure 2.1 shows the TRL of all HTGR concepts currently being developed with an expected net electric power output below 100 MWe [32]. Note, that there is a HTGR operational already with a TRL of 9 but this is a large land-based design that features a power output above 100 MWe.

It is difficult to find technical specifications of most HTGR designs. Although, for the U-Battery and the Holos-quad there are technical specifications readily available. In the second part of this report, information available for the Holos-quad reactor will be used for reference.

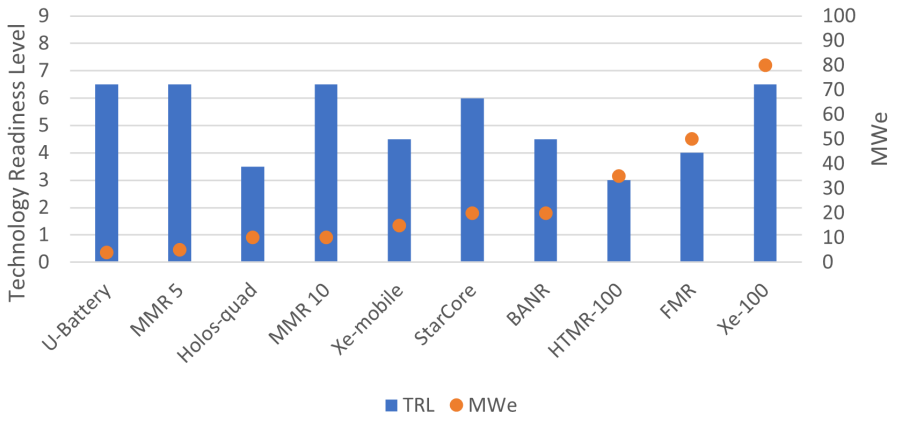

Figure 2.1: TRL and net power output for small (<100MWe) HTGR's currently being developed

2.3. Conversion from thermal power reactor to (electrical) power

This section covers the sub-question: How to convert the heat from the reactor into (electrical) power?

The on-board HTGR would be the source of energy in the form of heat. The heat energy has to be converted into mechanical energy. A generator converts mechanical energy into electrical energy. Power conversion can take place via three power cycle principles: Rankine, closed Brayton cycle and open Brayton cycle.

2.3.1. Rankine cycle

The steam turbine (Rankine cycle) has been applied for decades on board of PWR-powered vessels and is therefore well-developed and considered safe. However, a HTGR will have higher output temperatures compared to the Gen-II(I) PWR systems. These higher temperatures would require conditions beyond super criticality- given the nature of steam. To use a conventional steam power cycle, part of the heat should be directed away. Because such high temperatures are not beneficial to any other application on board. Thus, with regards to energy efficiency it is not recommended to connect a steam power cycle to a HTGR. As shown in table 2.1.

2.3.2. Brayton cycle

The Brayton cycle principle is about powering turbomachinery with a medium other than steam, such as helium (He), supercritical carbon dioxide (sCO2) or air. Different to steam, there is no phase change. Current HTGR designs typically feature the concept of a direct cycle or an indirect cycle. The indirect cycle can be closed- or open cycle.

The direct cycle

For a direct cycle, the coolant transferring the heat from the reactor directly flows through a power cycle. Figure 2.2 shows a sketch of such cycle. The figure shows a sketch of an inter-cooled cycle with a recuperator as this is studied to be more efficient, which will be elaborated on later in this subsection. In a HTGR, helium gas is the coolant transferring the heat from the reactor. Helium is a chemically inert- and non-reactive gas and follows the ideal gas law under a wide range of conditions. Therefore, it is possible to run the medium through turbo machinery directly. The main interest for the direct cycle originates from its potential to be very compact [1].

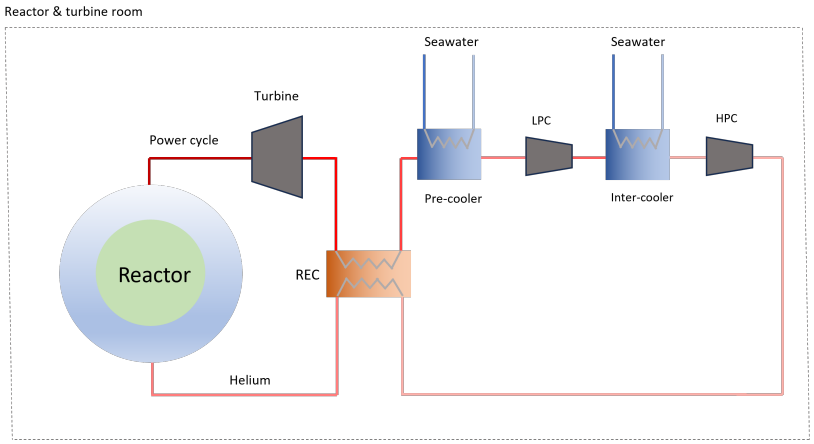

Figure 2.2: HTGR inter-cooled direct power cycle with recuperator sketch

Indirect cycle

The indirect cycle is about physically separating the primary coolant running through the reactor from the medium in the power cycle. The heat between the two different cycles is transferred in a so-called intermediate heat exchanger (IHX). There are different reasons to choose for an indirect cycle.

First, in the indirect-cycle it is possible to choose a different medium for your power cycle. Mediums commonly researched are helium, sCO2 and air. The prominent advantages of helium; medium technology maturity of helium turbine cycle, being an inert gas, high specific heat capacity and in line with increasing reactor outlet temperatures (i.e. increasing reactor outlet temperature favours the use of helium). Disadvantage of helium; very lightweight and thus subjective for tiny leaks in the system. The prominent advantages of using sCO2 would be; smaller equipment, greater efficiencies at lower temperatures. Disadvantages sCO2; corrosive, not inert, high pressure requirement and max. coolant temperature around 690 degree Celsius. The latter argument is important to take into account given the rising output temperatures of HTGR's. The advantage of using air in an open cycle: the ease of sudden heat release to the environment and the readily available knowledge in compressor- and turbo machinery technology. Disadvantage: lower- thermal conductivity and energy density of air, which would require large ducts and large volume flows in order to transport equal heat flux.

Second, even though helium is inert, using a different power cycle minimises the risk of contamination reaching the turbo machinery. In line with this, the consideration could be redundancy, safety, regulatory, flexibility and maintainability.

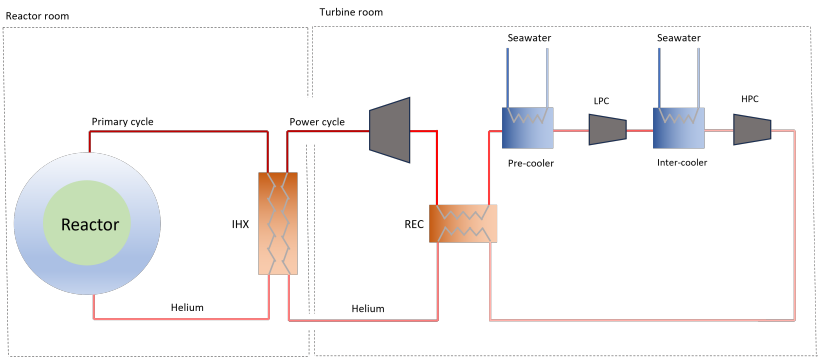

Figure 2.3: HTGR inter-cooled indirect power cycle with recuperator sketch

The closed-Brayton concept could yield overall cycle efficiencies up to around 50% [12] [13] [27] [8]. This percentage is considering high reactor output temperatures (VHTR level) together with a recuperator and inter-cooler embedded in the closed cycle. Efficiencies for the open Brayton cycle could reach 45%. As a reference, the Rankine cycle typically peaks around 35% [9][8]. Both the

closed- and open Brayton turbine system take up significantly less space compared to a steam turbine. See figure 2.4 for an illustrative comparison of size [34]. This is key to current very small modular reactor designs as the power conversion system can be easier embedded in the system as a whole. Therefore, the expected power-to-weight ratio of the Brayton cycle is higher, which will be favourable on board of a ship. Besides, being able to install the HTGR with the power conversion unit embedded in a 'one box' solution is potentially desirable from a cost- and technical perspective compared to a ship-specific steam installation - which is the case in today's fleet of nuclear-powered ships.

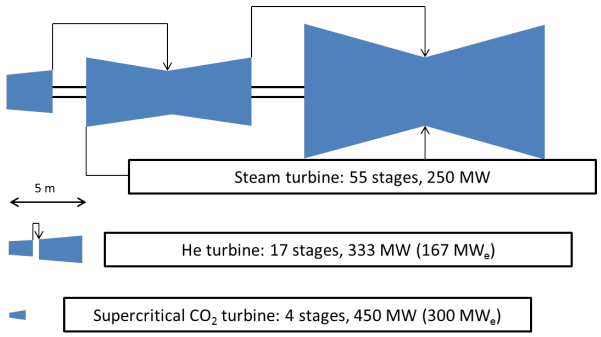

Figure 2.4: Schematic comparison size Rankine versus Brayton turbine [34]

2.3.3. Comparing the power conversion options

In order to understand the differences between the different power cycle suggested in this chapter, a comparison is made. Table 2.1 shows a comparison of the options discussed to convert heat from the HTGR into mechanical power. The comparison of different power cycle principles is performed based on: volume, weight, complexity, efficiency, cycle pressure range and max turbine inlet temperature. The differences are to be interpreted as indicative, rather than absolute.

Heat source	Reactor output temperature	Primary coolant	Power conversion method	Power cycle medium	Volume (system)	Weight (system)	Complexity (system)	Cycle efficiency	Pressure range power cycle	Max turbine inlet temperature
HTGR	750 - 950	Helium	Closed Brayton cycle	Supercritical CO2	++	+	-	++	80 - 300 Bar	700°C
				Helium	+/-	+/-	-	++	10 - 100 Bar	850°C
			Open Brayton cycle	Air	+/-	+/-	+	+	10 - 40 Bar	1500°C
			Rankine cycle	Steam	-	-	+	-	1 - 240 Bar	600°C

Table 2.1: Comparison of the different power cycles

Based on the comparison shown in table 2.1 the Rankine cycle is not preferred in combination with a HTGR. It requires a large and heavy installation. The system pressure is high, and cycle temperatures are below that of the HTGR output - resulting in a low cycle efficiency potential.

The sCO2 cycle has great potential to be compact and light and could feature high efficiencies. However, the cycle will operate at high pressures and the HTGR output temperature will be too high for the sCO2 power cycle - reducing cycle efficiency potential again.

The open Brayton cycle shows potential in combination with a HTGR. An open Brayton cycle is expected to bring fewer complexities at first. As air is readily available, the total system would not require complex handling, storage, sealing or processing systems that would be needed for other working fluids like helium or CO2. With respect to the turbomachinery itself, there is 200 plus years of experience in gas turbines which can be applied. The higher the output temperature of the reactor, the closer it gets to the inlet temperatures of conventional gas turbines today [19].

The closed Helium cycle shows great potential in combination with a HTGR in the future as well. It could yield a high cycle efficiency and the greater the output temperature of the reactor, the greater the cycle efficiency potential. The max pressure level would be significantly lower - max 100 bar - compared

to using supercritical CO2 or steam. Comparing it to the open air cycle, the turbomachinery would be more complex as the experience in helium turbomachinery is lower.

In short, both the open cycle- and the closed helium cycle concept show potential to be applied in combination with a on-board HTGR installation. The focus of this report will be on the closed helium cycle. Initially, both concepts were to be elaborated upon and compared but there has not been enough time to cover both entirely.

2.4. Control of a varying power demand

This section covers the sub-question: How to control a varying power demand?

To ensure safe, efficient and adaptive control of the power cycles discussed in this chapter, there are controlling systems required beyond reactor control only.

For the closed Brayton cycle there are different control methods discussed in various research. The four most promising control concepts appear to be: Valve control, heat source control, inventory control, and rotational speed control of turbo machinery [3] [40][26][29].

Valve control
Valve control is about controlling the valve position in a pipe and can be applied at different locations in the system. Via valves the mass flow can be controlled or diverted at different locations in the power cycle. It is also possible to enable a bypass of a stream by opening a valve. This is referred to as bypass control in this report. Different research about the HTGR direct helium cycles have discussed the potential of compressor throttling, turbine throttling and turbine bypass. The potential of each mechanisms depends on situation and affiliated purpose and none is ruled out yet. These control mechanisms are explained and researched in chapter 5.

Heat Source control
In research about the control mechanisms, reactor control is typically referred to as heat source control. Which is essentially about controlling the heat flux out of the HTGR. Reactor control is complex and requires significant knowledge about nuclear physics. This will not be the main focus in this research. Yet, the working principle and a simplification is discussed in section 3.1 and chapter 4.

Inventory control
The concept of inventory control is having an extra tank to which mass flow can partly be bypassed or from which extra mass can be taken. By controlling the helium inventory, the power output of the system can be adjusted. For example, increasing the helium inventory raises the pressure and mass flow rate, which can increase the power output. Conversely, reducing the helium inventory can decrease power output, which is useful in load-following scenarios where power demand fluctuates. Inventory control is explained and researched in chapter 5.

Rotational speed control
Rotational speed control of turbo machinery is about changing the rotational speed of turbo machinery in order to control power output. First, the rotational speed influences both the mass flow and the pressure ratio in the system and thereby the power output. This could also enable active prevention of surge or stall, which can both damage the machinery seriously. Thus, rotational speed control could allow the system to respond dynamically to changes in demand, regulate temperatures, and prevent operational issues like compressor surge/stall or mechanical stresses.

Research iterates that control mechanisms could improve load-following capability of HTGR power cycle[3] [40][26][26][29]. To determine the actual role these control mechanisms could fulfil in the closed power cycle, their function could be simulated in accordance with an actual transient load profile. The control mechanisms are simulated and tested in chapter 4,5 and 6.

2.5. A first iteration power train

This section covers the sub-question: What would a first iteration power train look like?

In continuation of the conclusions drawn in previous sub sections, a first-iteration on-board power cycle would either be a closed Brayton cycle with helium or an open Brayton cycle. For the closed Brayton cycle, both a direct and indirect cycle should be assessed. The closed cycle would be intercooled and would feature a recuperator to reduce the temperature in the compressors and thereby increase cycle efficiency - as explained in section 2.3. Considering the time and resources available, it decided to study the direct closed Helium cycle first.

Since 1960, the helium Brayton cycle has received significant attention, and fifteen closed Brayton cycle nuclear reactor systems have been operationalized all over the world, including nine helium Brayton cycle reactor systems [37]

The power train will consist of HTGR directly connected to the turbomachinery. The closed cycle will feature two compressors and one turbine. Next, it will have two cooling stages. The first one (IC1) before the low pressure compressor (LPC) and the second one (IC2) before the high pressure compressor (HPC). The power cycle also contains a recuperator to lower the temperature level of the helium in the compressors and to improve cycle efficiency. There are more options to configure this power cycle. For example, increasing the number of turbines. Which could be preferable from a sizing-, safety- and/or redundancy perspective. However, the single turbine set-up as described corresponds to a concept currently being developed: the Holos-Quad reactor [33]. As there is much detailed information available about this small HTGR concept, it is opted to use this as a first iteration power cycle. A sketch of the set-up can be found in appendix C.

3

System characteristics of an on-board HTGR installation

This chapter covers the sub-question: **How do the different sub-systems in the closed helium Brayton cycle influence the overall load-following performance of the power cycle?** For each sub-system at least the following aspects are discussed: Function, design and its role in the dynamic characteristic of the Brayton power cycle.

3.1. The High-Temperature Gas Reactor

3.1.1. Function

The function of the on-board HTGR is considered most crucial. The HTGR heats the helium by transferring the thermal energy generated by fission in the reactor core to the helium as it circulates through the core.

3.1.2. Design

There are two main types of HTGRs: The pebble bed reactor (PBR) and the prismatic block reactor. Both reactor types use helium as a coolant. The prismatic block reactor features hexagonal graphite blocks with em-bedded fuel compacts containing TRISO-coated particles and the pebble bed reactor features spherical fuel elements with TRISO-coated particles. While both PBR- and prismatic block designs are used in HTGRs, there appears to be more interest in pebble bed reactors today, particularly in China. This is due to their operational flexibility, safety features, and ease of coolant flow. However, prismatic block reactors continue to be relevant and are favoured for their higher power density and structural stability.[1] [32]. Table 3.1 shows a comparative overview between the two type of reactors.

Feature	Pebble Bed Reactor (PBR)	Prismatic Block Reactor
Fuel Type	Spherical fuel elements (pebbles) with TRISO-coated particles	Hexagonal graphite blocks with embedded fuel compacts containing TRISO-coated particles
Coolant	Helium gas	Helium gas
Design	Randomly packed pebbles in the reactor core	Stacked graphite blocks with drilled coolant channels
Fuel Handling	Continuous or batch-wise online refueling	Batch-wise refueling
Core Structure	Dynamic with moving fuel elements	Static with fixed fuel elements
Thermal Conductivity	High due to loose packing and direct helium flow	High due to graphite blocks and helium flow
Power Density	Generally lower	Generally higher

Table 3.1: Comparison of pebble bed reactor and prismatic block reactor

With respect to application on board, the operational flexibility of continuous refuelling of the pebble bad reactor could be an advantage. However, this refuelling could - and potentially is preferred to - coincide with mandatory dry-docking every 5 years. For the prismatic block reactor, the higher power density could be favourable, considering limited space on board of the vessel. Finally, the fuel being statically positioned is preferred given the motions of a ship. In this study the prismatic block reactor designed for the 5.5 MWth Holos-Quad reactor is picked and used for reference [27].

3.1.3. Dynamics

The reactor plays an important role in the dynamic characteristics of the Brayton power cycle. Reactor controls should control the core reactivity to keep the fission under control during variations in thermal conditions of the coolant or a desired change in reactor output. There are multiple mechanisms inside the core that play a role in the net reactivity of the HTGR. Four types of mechanisms that play an important role in the fission reaction are:

- Control rods - These can be inserted or withdrawn from the reactor core to absorb neutrons and control the fission rate. A typical material for a control rod is boron as it has a high neutron absorption capability.
- Burnable poisons - additional materials incorporated into the fuel to absorb excess neutrons.
- (Movable) reflectors - Reflectors are materials surrounding the reactor core that reflect neutrons back into the core, increasing the likelihood of fission reactions.
- Temperature feedback - The temperature and pressure of the helium influence the core's temperature. For example, increased flow or pressure can remove more heat, lowering the core temperature. This will actually lead to an increased reactivity due to the negative temperature coefficient. Evenly, an increase in temperature of the coolant will actually lead to an automatic decrease in reactivity. The Doppler effect is a key part of the negative temperature coefficient. As the fuel temperature rises, the uranium atoms vibrate more, causing the absorption cross-section for neutrons to increase. This reduces the number of neutrons available for causing fission and thus decreases the reactor's power output.

The concept of temperature feedback means that the reactor's dynamics are sensitive to changes in the heat flux of the coolant as it flows through the core. In other words, the combination of temperature, pressure and mass flow of the helium coolant through the core influences the reactivity. The reactor power level is essentially a balance between temperature feedback by control rods and reflector against the temperature feedback from the fuel and moderator.

To be able to both understand and define the dynamic limits of varying the thermal power output of the HTGR, it is essential to have extensive knowledge about reactor kinetics. This knowledge should cover at least; the neutron life cycle, reactivity control, delayed neutrons, reactor kinetics equations, heat transfer dynamics, transient behaviour, fuel burnup and radiation shielding. However, any matter related to reactor kinetics is outside the scope of this report.

It was found that continuous load following has an impact on the xenon concentration inside the reactor. At higher power levels, the neutron flux increases, leading to higher rates of xenon burnout, reducing its concentration. At lower levels the xenon burnout is slowed down and the concentration will increase. The xenon concentration does influence reactivity and thereby the transient load capability of the system. Despite this, the change in xenon concentration is not expected to influence the outcomes of this research given the short duration of the transients [27]. However, this effect should be included in determining final feasibility of adapting to repetitive power transients.

Research about defined load-following limits of small HTGR is limited. Different sources suggest maximum power ramp rates between 5- and 10% of max power per minute [17][41] [1]. In addition, essential clarification is often missing as well. Such as; does it refer to reactor thermal power or net cycle output power? What are the factors limiting the change rate? What is the effect of repeating the same transient multiple times after each other? What is the effect on system and material lifetime? How does ramp-up differ from ramp-down? Despite these uncertainties, it is known that high- and/or strongly fluctuating power shifts will reduce the lifetime of the reactor and should therefore be minimised in case possible.

According to the International Atomic Energy Agency (IAEA), typical ramp-up and ramp-down rates for HTGRs are defined as follows:

- ”Ramp-Up Rate: Generally, HTGRs can increase their power output at a rate of up to 5% of full power per minute. This controlled ramp-up rate helps manage thermal stresses and ensures that the reactor components, including the fuel and moderator, can safely handle the increase in heat load.” [1]
- ”Ramp-Down Rate: HTGRs can decrease their power output more rapidly, typically up to 10% of full power per minute. The faster ramp-down rate is crucial for safety, allowing the reactor to quickly reduce power in response to operational needs or emergencies, thereby reducing thermal and mechanical stress on the reactor components.”[1]

Thus, the exact limits on continuous load-following for a small HTGR are difficult to obtain and - to some extend - still undefined today. Considering the aforementioned, the required reactor thermal power will be calculated for different transients in this report and the power change rate will be monitored. In analysing these change rates, the suggested max change rates as discussed above will serve as a reference.

The slow response of a reactor is largely due to its large thermal mass. This will be calculated and included in the simulations. The calculations for thermal mass are shown in appendix A.1.

Also, it will be required to set a minimum on the reactor thermal power during normal operation. This ensures that the reactor operates efficiently and that the decay heat can be managed safely. The IAEA and other regulatory bodies mention that a minimum operational power level around 10-20% of full power is a common practice to ensure safe and efficient operation. 20% is common practice for reactors operational today and therefore a conservative assumption [1][7].

3.2. Heat exchanger

3.2.1. Function

The heat exchanger plays an essential role in nuclear-based power generation. It allows for the exchange of heat between different mediums and/or cycles in a nuclear power cycle. Table 3.2 shows 3 main roles a heat exchanger fulfils in a typical HTGR cycle.

Name	Abbrev.	Function
Intermediate heat exchanger	IHX	Transfer heat between the primary cycle coolant and the second cycle coolant
Cooling Heat exchanger	CHX	Transfer heat from a coolant to the environment (atmosphere or body of water)
Recuperator	REC	Transfer after-turbine heat to the before-reactor stream

Table 3.2: Heat exchanger functions in a (very) high temperature gas reactor

By effectively transferring heat from the HTGR to the Brayton cycle, the heat exchanger plays a key role in optimising the cycle's thermal efficiency. The efficiency of the Brayton cycle is directly related to the temperature difference between the heat source (input from the HTGR) and the heat sink (where the working fluid is cooled before being compressed and reheated). However, any type of heat exchanger will induce some flow resistance. This resistance is to be overcome by the compressors in this case and thus plays a role in overall cycle efficiency.

3.2.2. Design

There are different types of heat exchangers used in the nuclear industry. Heat exchangers are typically categorised based on their type and flow arrangement. Each type of heat exchanger has its own characteristics. The same heat exchanger type can have different flow arrangements, which subsequently influences its performance and efficiency. The three general flow-arrangements are: Parallel-, counter, and cross-flow. Therefore, choosing a heat exchanger should depend on the intended application.

Table 3.3 lists four types of heat exchangers most-commonly discussed in the nuclear industry [4] [24]. Because the heat-exchangers have to be installed on board of the vessel, the table also contains an indicative comparison on weight- and space required for each type.

In addition to the required duty, the size of the heat exchanger also depends on: characteristics of the medium(s), the flow arrangement, conditions, materials - amongst other aspects. However, the weight- and spatial aspect is discussed first.

Type	Name	Abbreviation	Weight / Duty	Area density
			(tonnes/MW)	(m^2/m^3)
Tabular	Shell & tube	STHE	13.5	75
Tabular	Helical coil	HCHE	6	80
Plate	Printed Circuit	PCHE	0.2	1250
Plate	Plate (& fin)	PFHE	0.2	800-1500

Table 3.3: Indicative size of different heat exchangers used commonly in the nuclear industry [2] [36]

The recuperator duty is at least two times the net electrical output of the HTGR-cycle [13][36]. For example, when a vessel would require 20 MWe of installed power, the required weight for a shell-and-tube recuperator alone would exceed 540 tonnes. This is unfavourable on board of a dredging vessel. This contrasts with the PCHE and the PFHE, which are both very compact heat exchangers. Thus, the PCHE and PFHE appear to be more feasible with respect to weight.

Literature research shows that the PCHE types have been studied most widely in HTGR concepts

[15].Therefore, the PCHE type will be the initial heat exchanger choice for the recuperator and intermediate heat exchanger.

The heat exchanger type for the inter-coolers will be a shell and tube heat exchanger. There are different reasons for this. First, when cooling helium gas in the tubes with cold water in the shell, the heat capacity ratio is favourable which means the heat exchanger would not have to be the same size as discussed for the recuperator. Thus, size and volume is calculated to be acceptable. Second, for the pre- and inter cooling heat exchanger on board of a ship, the effectiveness is expected to be less relevant compared to the recuperator. For the cooling heat exchangers, the temperature of the water will be lower than the coolant in the Brayton cycle at all times. Additionally, the availability of cooling water is unlimited and mass flow can be increased at relatively low energy cost. This means a simple, robust and low maintenance shell and tube heat exchanger can be chosen. Third, directly using seawater in a PCHE heat exchanger is not possible.

3.2.3. Heat exchanger heat transfer capacity

To analyse heat transfer in an exchanger, it is possible to relate the heat transfer rate q, heat transfer area A, heat capacity rate C of each fluid, overall heat transfer coefficient U, and fluid terminal temperatures. Two important relations comprise the entire thermal design procedure [31]:

$$q = q_j = \dot{m}_j \Delta h_j = (\dot{m} c_p)_j \, \Delta T_j = (\dot{m} c_p)_j \, |T_{j,i} - T_{j,o}| \tag{3.1}$$

$$q = UA\Delta T_m \tag{3.2}$$

Equation 3.1 is the relationship from thermodynamics which relates the heat transfer rate q with the enthalpy rate change for an open non-adiabatic system for each of the two fluids (j=1,2). The relation to temperature is valid when considering single-phase gas. Equation 3.2 describes the convection-conduction heat transfer phenomenon in a heat exchanger according to the log mean temperature difference method (LMTD). This method is commonly used to calculate the heat transfer for steady-state- and continuous-flow heat exchangers [31]. ΔT_m is the mean-temperature difference between the two gasses according to equation 3.3.

$$\Delta T_m = \frac{\Delta T_1 - \Delta T_2}{\ln\left(\frac{\Delta T_1}{\Delta T_2}\right)} \tag{3.3}$$

Where ΔT_1 and ΔT_2 are the temperature differences at the two ends of the heat exchanger.

In the situation where the temperature profiles are not known, the $\epsilon - NTU$ method is widely used to determine the heat transfer rate [31] [21]. The basic concept of this method starts with equation 3.4 and 3.5:

$$q = \epsilon q_{max} = \epsilon C_{\min} \left(T_{h,i} - T_{c,i}\right) = \epsilon C_{\min} \Delta T_{\max} \tag{3.4}$$

$$\epsilon = \phi(\text{NTU}, C_r, \text{flow arrangement}) \tag{3.5}$$

Thus, the heat exchanger effectiveness: (ϵ) - or sometimes referred to as 'thermal efficiency' - is dependent on the NTU, C_r and flow arrangement. NTU stands for 'Number of transfer units'. (ϵ), NTU and C_r are non-dimensional. NTU and C_r are defined as:

$$C_r = \frac{C_{\min}}{C_{\max}} = \frac{(\dot{m} c_p)_{\min}}{(\dot{m} c_p)_{\max}} = \begin{cases} \frac{(T_{c,o} - T_{c,i})}{(T_{h,i} - T_{h,o})} & \text{for } C_h = C_{\min} \\ \frac{(T_{h,i} - T_{h,o})}{(T_{c,o} - T_{c,i})} & \text{for } C_c = C_{\min} \end{cases} \tag{3.6}$$

$$\text{NTU} = \frac{UA}{C_{\min}} \tag{3.7}$$

$$UA = \frac{1}{R} = \frac{1}{R_{h,convection}} + \frac{1}{R_{h,fouling}} + \frac{1}{R_{wall}} + \frac{1}{R_{c,fouling}} + \frac{1}{R_{c,convection}} \tag{3.8}$$

$$R_{i,convection} = (hA)_i \qquad [i = c \vee i = h] \tag{3.9}$$

$$R_{i,fouling} = (h_f A)_i \qquad [i = c \vee i = h] \tag{3.10}$$

$$R_{wall} = \frac{\delta_w}{k_w A_w} \tag{3.11}$$

Equations 3.8 to 3.11 show how the overall heat transfer coefficient 'U' over heat transfer surface 'A' is a function of the convection-, fouling- and wall thermal resistance. h and h_f in equation 3.9 and 3.10 are the heat transfer coefficient and the fouling coefficient. In equation 3.11, δ_w is wall plate thickness, k_w is the thermal conductivity of the wall material.

Finally, the relationship between ϵ, C_r and NTU depends on the flow arrangement - such as counter flow, parallel flow, or cross flow. In practice, these relationships can be found in heat transfer textbooks or engineering references, often in the form of charts or graphs that simplify the process of determining effectiveness for various NTU and C_R [31]. A basic overview of these relations can be found in appendix B.

3.2.4. Heat exchanger effectiveness

The recuperator has a prominent effect on the overall cycle efficiency. Therefore, the recuperator should be designed to have a high thermal effectiveness. In fact, below a certain effectiveness it would not make sense to include a recuperator in the cycle because the recuperator is there to allow for a more efficient compression cycle. An intercooled cycle (IC) with a recuperator would increase the total cycle efficiency by approximately 3% compared to a simple cycle without IC and a recuperator [11] [13]. Also, the recuperator should be compact enough to be able to fit on board the vessel.

3.2.5. Heat exchanger material and dynamics

The type of material that a heat exchanger is made of has a impact on its performance. Aside differences such as weight, corrosion resistance and mechanical strength, each material also has its own thermal conductivity characteristic. A greater thermal conductivity could mean less required heat transfer area. Also, the thermal mass is a function of the thermal conductivity which influences the transient response of the heat exchanger.

Most importantly, the material of the heat exchanger should be chosen upon the operating circumstances and type of mediums flowing through. The material should be able to withstand the expected (fluctuation of) temperatures and pressures. Heat exchangers in radiation affected area's, should also be resistant to radiation.

There are many different materials to choose for a heat exchanger. Table 3.4 shows an indication of the effect of the different type of materials used in heat exchanger. It is common to divide the materials in 3 general groups: stainless steel, titanium based and nickel based. From each group, one exemplary type is picked, which reflects a common type used in PCHE's [25]. It strikes that stainless steel shows reasonably similar characteristics in comparison to the other two - which are significantly more expensive. CP-grade titanium has a lower density which allows for a lighter heat exchanger and therefore a lower thermal mass.

Property	SS316	CP Grade Titanium (Grade 2)	Alloy 800H/T
Thermal Conductivity	~16 W/m·K	~17 W/m·K	~11 W/m·K
Density	~8.0 g/cm^3	~4.51 g/cm^3	~7.94 g/cm^3
Specific Heat Capacity (c_p)	~500 J/kg·K	~520 J/kg·K	~460 J/kg·K
Cost	$2-3/kg	$10-20/kg	$20-30/kg
Creep Resistance	Good	Moderate	Excellent
Corrosion Resistance	Excellent	Excellent	Excellent
Oxidation Resistance	Good	Good	Superior

Table 3.4: Comparison of properties for SS316, CP Grade Titanium (Grade 2), and Alloy 800H/T. [25]

The closed- and open- Brayton cycle concept requires one or more heat exchangers in the power cycle. The transient response to a sudden fluctuation in temperature or heat flux in a heat exchanger depends on the thermal mass of the walls. The wall thermal mass is the heat required to raise the wall temperature by one degree and is calculated via equation 3.12. m_{wall} is the total mass of the heat exchanger walls and depends on the size- and type of heat exchanger. Cp_{wall} is the specific heat capacity of the wall material.

$$Thermalmass = m_{wall} * Cp_{wall} \tag{3.12}$$

Both the (inner) dimensions- and configuration of the heat exchanger and the flow properties of both flows, influence the pressure drop over the heat exchanger. The lower the pressure drop over the heat exchanger, the higher the efficiency of the power cycle. This is because the pressure drop would have to be compensated by the compressor - which induces extra work. Yet, the layout of the heat exchanger should be such that heat transfer is optimal. For the purpose of this study the aim was to simulate the heat exchanger such that is features the heat exchanger effectiveness similar to the 5.5 MWth Holos-Quad concept [27]. For that, the layout and dimensions were changed by means of iteration until acceptable effectiveness was achieved. The pressure drop over the heat exchanger is simulated using a constant loss coefficient according to equation 3.13 and 3.14. The pressure loss coefficient (ξ) was chosen such that the pressure drop for helium over IC1, IC2 and the recuperator are approximately 0.15, 0.15 and 1.14 bar at nominal conditions. This is similar to the pressure drops described for the Holos-Quad design [27] and in proximity to typical pressure drops mentioned in other research as well [22] [6].

$$if Re < 4000, p_{in} - p_{out} = \xi \mathrm{Re}_L \frac{\dot{m}\mu}{2D_H \rho_{A\mathrm{Min}}} \tag{3.13}$$

$$if Re > 4000, p_{in} - p_{out} = \xi \frac{\dot{m}\,|\dot{m}|}{2\rho_{A\mathrm{Min}}^2} \tag{3.14}$$

To get a feeling of the impact of thermal mass, the thermal delay of the recuperator is assessed. Figure 3.1 shows the response to an imaginary temperature increase of the helium coolant in a 10 MW recuperator for the 3 different materials. The mass flows on both sides is equal.

The figure illustrates how different materials with varying thermal masses affect the thermodynamic response of the recuperator. Materials with higher thermal mass (like SS316) exhibit slower temperature changes, making the system more stable but slower to adjust to load changes. Materials with lower thermal mass (like Titanium) show faster responses, making them better suited for applications requiring rapid load-following but potentially introducing more temperature variability.

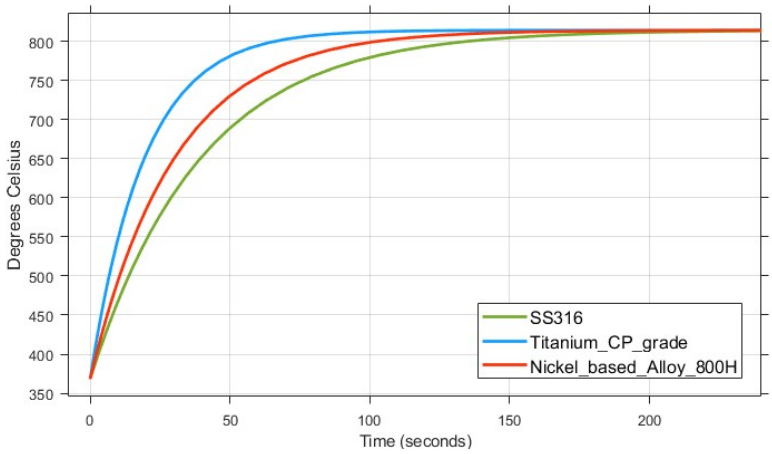

Figure 3.1: Effect thermal mass on thermodynamic response recuperator [1]

Thus, thermal mass has a an impact on the transient behaviour of the heat exchangers in the cycle, influencing how quickly the system can adjust to changes in operational conditions, while at the same time mitigating the effect of abrupt heat fluxes. Nonetheless, the effect will be about a few seconds maximum for typical transients.

3.3. Inter-cooling

3.3.1. Function & dynamics

Inter-cooling refers to a process used in multi-stage compression systems, where the working fluid is cooled between stages of compression. Cooling before the low pressure compressor is typically referred to as ”Pre-cooling” and the cooling between the low pressure compressor and the high pressure compressor is typically referred to as ”Inter-cooling.” Inter-cooling the helium before it enters the compressors in the closed Brayton power cycle has different functions:

First, it allows for control of the temperature of the gas before it enters the compressor. Controlling the temperature at the compressor inlet is required for consistent performance of the compressor. This is key in ensuring system stability and sustainability of the compressor equipment. Especially when considering the high RPM levels in the helium turbomachinery in combination with transient load fluctuations in the system. Power control mechanisms - which will be discussed in chapter 5 - could lead to an increased heat flux flowing back to the compressors. This heat flux can be compensated by increasing cooling capacity. Thus, inter-cooling plays an important role in power control as well.

Second, in addition to regulating the temperature, it allows to lower the temperature of the gas before it enters the compressor. When the temperature of the gas is lowered, the density increases which allows for a higher mass flow at a given volume, which improves efficiency of the compressor. More importantly, compressing a gas at a lower temperature requires less energy. However, the reduction in energy required to compress the gas to a certain pressure should offset the increased pressure resistance and additional loss of heat. The latter is after all the source of power in this cycle. Therefore, a recuperator is required. Without a recuperator, inter cooling does not make sense from an energy efficiency standpoint. As mentioned before, an intercooled cycle (IC) with a recuperator would increase the total cycle efficiency by approximately 3% compared to a simple cycle without IC and a recuperator [11] [13].

Third, inter-cooling allows to cool away a surplus of energy by the reactor when certain ”bypass” control mechanisms are utilised. This will be discussed in chapter 5.

Thus, an intercooled recuperated closed Brayton cycle configuration enables enhanced control of the compressor inlet temperature in transient load behaviour and thereby guaranteeing a steady compressor operation at a lower temperature and at a higher efficiency. In addition, it allows to cool away any increased heat flux diverted or induced via some control mechanisms.

3.3.2. Design

When cooling helium with (sea)water the heat capacity ratio is favourable such that the heat exchange is more efficient - as explained in subsection 3.2.2. Thus, the size and volume of the heat exchanger can be limited. Next, the effectiveness of the cooling heat exchangers is less important because the cooling flow can easily be adjusted to compensate for an increased heat flux. Thus, it was opted to design two shell and tube heat exchangers for this purpose. The design is done via the NTU-Method explained as explained earlier in section 3.2. Detailed design properties can be found in appendix B.

3.4. The compressor and turbine

3.4.1. Function

The compressor's primary function is to increase the pressure of the working fluid (helium) before it enters the reactor. The turbine's primary function is to extract energy from the high-pressure, high-temperature helium after it has been heated by the reactor. This energy is converted into mechanical work, which - in this case - will be used to drive the on-board generator.

3.4.2. Design

The design of the turbomachinery influences the performance of the power cycle. The design of a compressor or turbine for helium is different than for air. This is due to the difference in gas properties. Table 3.5 shows the key differences in properties between Helium and Air. First, Helium is the second lightest element in the periodic table which brings complexities. The turbomachinery needs to constructed differently and potential leakage is to be accounted for.

Second, helium is difficult to compress due to its thermodynamic properties. Therefore, a helium compressor would require additional stages to compress helium to a certain pressure ratio compared to an air compressor. This leads to more slender rotors which is unfavourable with respect to rotor dynamics. Besides, this lowers the power density of the machinery. To overcome this, highly loaded design methods of helium compressors have been proposed. This design technique is to significantly improve helium compressor performance and make it able to deal with a higher load in a single stage. Nevertheless, all the helium compressors constructed today still have a high number of stages. The difficulty of helium compression is still the key challenge in the practical application of helium compressors [37].

For nitrogen and air the blade peripheral velocity is restrained by material strength and sonic speed, while for helium by material strength only, since helium sonic speed is about three times of nitrogen or air [39].

The blade profile is another key aspect of the turbomachinery design. The air compressor has accumulated a set of blade profiles which are useful for the air compressor design from low to high speeds. But as the specific heat of helium is five times that of air; the isentropic index is 1.2 times that of air; and the sound velocity is three times that of air, the conventional air foil design cannot be used directly in the helium compressor design. Therefore, it would be necessary to develop a set of helium blade profiles with lower losses and higher loads.

Property	Air	Helium
Molecular Weight	28.97 g/mol	4.00 g/mol
Specific Heat Ratio (γ)	1.4	1.66
Density (ρ)	$\frac{P}{287 \cdot T}$ (higher)	$\frac{P}{2077 \cdot T}$ (lower)
Specific Heat Capacity (c_p)	1005 J/(kg·K)	5193 J/(kg·K)
Specific Gas Constant (R)	287 J/(kg·K)	2077 J/(kg·K)
Speed of Sound (a)	$\sqrt{1.4 \cdot 287 \cdot T}$ (Lower)	$\sqrt{1.66 \cdot 2077 \cdot T}$ (higher)
Mass Flow Rate at Choke ($\dot{m}_{choke}$)	$\propto \frac{P \cdot A}{\sqrt{T}} \cdot \sqrt{\frac{1.4}{287}}$ (higher)	$\propto \frac{P \cdot A}{\sqrt{T}} \cdot \sqrt{\frac{1.66}{2077}}$ (lower)

Table 3.5: Comparing the parameters that influence the design of an air and helium compressor.

3.4.3. Dynamics

The turbomachinery in a closed helium Brayton cycle plays a crucial role in managing load-following in a high temperature gas reactor. Both the compressors and the turbine(s) would allow a faster dynamic response than the reactor itself because it directly effects the high enthalpy flow. This allows the system to follow load changes more quickly by altering the flow rate of helium through the compressor and turbine. However, the change of mass flow, pressure and temperature will affect the the heat removal from the reactor core.

The rotating parts of the compressors and the turbine(s) also introduce a rotational inertia in the system. This could be advantageous as it stabilises small short-term fluctuations in load demand, smoothing out rapid changes in power output. Yet, flow disturbances through the compressors and turbine(s) should be minimised at all times as this can damage the structural integrity of the blades, given the high RPM requirements. The Holos-Quad design [2] features 2 compressors with a rotational speed of 15,000 RPM [27].

Next, surge, stall and choke in the turbomachinery is to be avoided at all time. Stall occurs when the mass flow rate is too low compared to the angle of the blades which will result in flow separation. It will reduce efficiency and cause vibrations and instability. When stall is not controlled, it could lead to surge. Surge is caused by a complete breakdown of flow through the compressors. The flow reversal will make the flow oscillating in the compressor and will damage components due to these high pressure fluctuations and vibrations. The effect on the power cycle will be a sudden pressure drop. To overcome surge, the rotational speed should be reduced. Choke occurs when the mass flow reaches sonic velocity and no further increase in mass flow is possible. Comparing this to surge, choke would not cause large instability in the system. Yet, it would limit the pressure ratio and the flexibility of the system to handle a potentially required higher mass flow.

To visualise the concept of surge and choke, figure 3.2 shows an indicative sketch of an axial compressor map with the surge and choke lines [42].

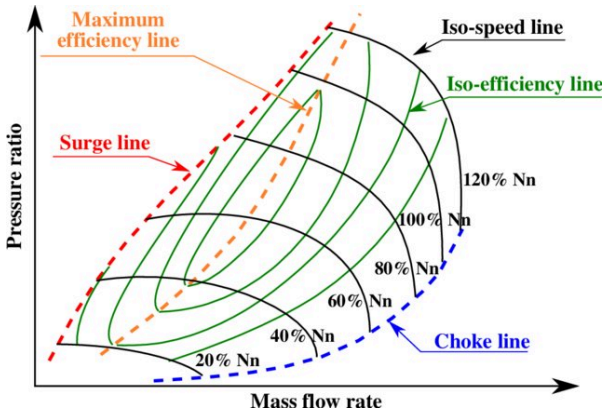

Figure 3.2: Schematic performance characteristic map for an axial compressor [42]

Although the characteristics of helium turbomachinery has been studied widely, it was found difficult to obtain actual valid compressor and/or turbine maps. It was found that detailed information remains with manufacturers and/or foreign countries that have operated - or are currently operating - HTGR's, such as in China.

In short, the gas properties from helium differ to that of air. Therefore, the compressor and turbine map will be different and thus the dynamic characteristic could be different. Table 3.6 summarises some key differences in the characteristics of the turbomachinery.

[2] See the design concept of this 10 MWe HTGR SMR in Appendix C

Property	Air compressor/turbo	Helium compressor/turbo
Surge Line Gradient	Steeper	Shallower
Pressure Ratio Behaviour	Increases rapidly with mass flow rate near surge limit	Increases more gradually with mass flow rate near surge limit
Velocity for Same Mass Flow Rate	Lower compared to helium	Higher compared to air
Choke Velocity (V)	At lower speed	At higher speed (due to higher speed of sound)
Rotational speed for certain pressure ratio	Lower	Higher

Table 3.6: Influence gas properties on the turbomachinery maps

3.5. Additional systems

Next to the HTGR, there could be other auxiliary sources of power or systems to improve operational flexibility and/or performance of the HTGR-powered vessel. For example: back-up power by diesel generators and/or batteries. This would also be essential with respect to redundancy and emergency reasons.

This report is about the power flexibility of the closed Brayton cycle connected to a HTGR and therefore the potential role of other auxiliary system possibilities is not discussed.

However, to better quantify load-following delays during transient dynamics, it will be calculated how much battery power would be required for power-take-in and power-take-off in order the realise the suggested power demand.

3.5.1. Batteries

A battery system on board a ship is typically referred to as a marine energy storage system (ESS). The ESS could deliver additional electrical power or receive a surplus in electrical power - assuming sufficient battery capacity. Lithium-ion batteries - which are commonly used - can typically handle high discharge rates to meet peak power demands or perform peak shaving.

Having an energy storage system (ESS) on board a HTGR-powered TSHD could bring these advantages as well. The ESS can supply additional power when the Brayton power cycle cannot meet the ship's power demand. This capability is useful for peak shaving and handling sudden and/or rapid increases in power demand. By assisting the balance between power supply and demand, the ESS could improve reliable operation. In addition, the use of the ESS could improve the transient load handling characteristic of the TSHD.

However, this report is about the potential of different control mechanisms in a Brayton power cycle to handle a varying power demand. Therefore, the initial function of the ESS will be to supply additional power at times when the power supplied by the Brayton power cycle - using the limits discussed in chapter 6 - cannot match the power demand. In addition, the ESS could store energy in case a surplus in power supplied by the Brayton cycle is experienced - under the condition of sufficient reserve capacity.

3.6. Chapter conclusion

This chapter explained the function of the different sub-systems that collectively form the closed Brayton power cycle connected to a high temperature gas reactor. In addition, initial design trade-offs are discussed and the influence of each sub-system on the dynamic capabilities of the power cycle are discussed.

First, it would be preferred to have a prismatic block reactor on board given it high power density and structural stability. Reactor power ramping rates should be minimised to reduce the impact on the materials and kinetic integrity of the reactor. When possible, ramping rates should be limited to a maximum of 5% for ramp-up and 10% for ramp-down. The large thermal mass of the reactor is what makes the reactor slow in power transients and should be included in the simulation.

Second, the heat exchangers play a key role in optimising the cycle's thermal efficiency and ensur-

ing thermodynamic stability where required. Given the requirement for high efficiency, fast thermal response and on-board weight constraints, a PCHE-type heat exchanger is picked for the recuperator. The heat exchangers used for the pre-cooler and inter-cooler can be more simple and robust, such as a shell-and-tube. The heat capacity ratio is favourable which reduces the required size of the heat exchanger. It was also shown how the thermal mass of the recuperator causes a small delay in thermodynamic response. Nevertheless, it can also assist in stabilising heat flux oscillations.

Third, an intercooled recuperated closed Brayton cycle configuration enables enhanced control of the compressor inlet temperature in transient load behaviour and thereby guaranteeing a steady compressor operation at a lower temperature and at a higher efficiency. In addition, it could cool any increased heat flux diverted or induced by control mechanisms

Fourth, both the compressors and the turbine(s) directly impact the pressure level and flow rates in the power cycle. Thereby, they play a crucial role in both sustaining a certain power level and adapting to a change in heat flux. The different gas properties of helium require a different design to the turbomachinery compared to conventional gas turbines. In transient power scenario's, the turbomachinery should be operated such that high efficiency is maintained and surge, stall or choke is avoided.

4

Model description

This chapter explains the thermodynamic model of the Brayton power cycle that was created in this study. The goal of the model is to be able to simulate; the thermodynamic processes of the suggested closed Brayton cycle; the effect of different control mechanisms; the thermodynamic effect of power transients and the overall load following characteristic of the suggested power cycles.

4.1. Nominal conditions selection

To study the characteristics of the closed direct helium power cycle - as discussed in chapter 2 - the thermodynamic and aerodynamic behaviour of such cycle is simulated. The 22 MWth Holos-Quad HTGR concept will form the design basis of the cycle [33]. A figure of the Holos-Quad concept is attached in appendix C.

The Holos-Quad reactor was chosen as reference for two reasons. First, for this design it was possible to obtain much detailed information. Second, because the nominal thermodynamic properties of the Holos-Quad are in close proximity to optimised conditions for such intercooled recuperated Brayton cycle as discussed in other studies [39] [13].

4.2. Methodology

First, each sub-system in the Brayton power cycle is built and tested individually. Each sub-system was built such that it would feature the same nominal conditions as the Holos-Quad concept.

Second, the different sub-systems are connected, creating a closed loop. Third, different control mechanisms are created and added to the simulation in order to study their effect on the power cycle. These control mechanisms are introduced in chapter 2 and described extensively in chapter 5. The thermodynamic model presented in this study was created using Matlab Simulink software.

By using the Matlab Simscape environment within Matlab it was sometimes possible to use existing code that allowed for accurate modelling of gas systems. The equations behind each model are elaborated on either in this chapter or in appendix A.

The table below shows a summary of the closed helium Brayton cycle that was simulated in this report.

Description	Value	Unit
Reactor thermal power	5.5	MWth
Heat source temperature	850	°C
LPC pressure ratio	1.41	-
LPC inlet pressure	3.5	MPa
LPC inlet temperature	40	°C
HPC inlet pressure	4.9	MPa
HPC pressure ratio	1.43	-
LPC & HPC mechanical efficiency	80-87.5	%
LPC & HPC isentropic efficiency	80-87.5	%
HPC & HPC rotational speed	15000	RPM
Turbine mechanical efficiency	98	%
Turbine isentropic efficiency	90	%
Turbine rotational speed	6000	RPM
Flow rate through cycle	4.08	kg/s
Plant thermal efficiency	44.4	%
Pre-cooler effectiveness	89.8	%
IC effectiveness	83.2	%
Pre-cooler cooling nominal	120	m3/h
Inter-cooler cooling nominal	120	m3/h
Recuperator effectiveness at nominal	0.94	%
Net generated output	2.45	MWe
Working fluid	helium	

Table 4.1: Nominal conditions power plant

4.3. Model limitations and assumptions

The following assumptions and/or limitations apply to the simulation performed:

- The helium gas is modelled as a perfect gas.
- Each pipe or sub-system - except for those with intentional heat exchange - is thermally isolated, with no heat loss to the environment. Because the transient heat flux simulation are relatively fast (seconds to minutes), this is not expected to have a significant influence on the results.
- The required power to be delivered by the reactor to the coolant is calculated purely from a thermal hydraulic perspective. An additional neutronics transients analysis is required to investigate whether the net reactivity produced in the fuel inside the reactor could actually oppose the feedback reactions caused in a specific situation. Such as: fuel temperature-, graphite matrix temperature and xenon reactivity- feedback. When the difference between net reactivity and reactivity feedback's is below the maximum drums reactivity in the core - the reactor can safely handle a transient situation.
- Pipe walls are rigid.
- Effect of gravity not included
- Fluid inertia is negligible
- The used gas properties of helium are listed in table 4.2.

Gas specification	Value	Unit
Specific gas constant	2.0771	kJ/kg/K
Compressibility factor	1.0005	-
Reference temperature for gas properties	273	K
Specific enthalpy at reference temperature	1418	kJ/kg
Specific heat at constant pressure	5.193	kJ/(K*kg)
Dynamic viscosity	18.7	s*µPa
Thermal conductivity	0.151	W/(K*m)

Table 4.2: Gas properties helium

Continuity equations

In each sub-system conservation of mass applies (eq. 4.1) and the energy balance is computed using equation 4.2.

$$\dot{m}_A + \dot{m}_B = 0, \tag{4.1}$$

$$\Phi_A + \Phi_B + (P_{\text{fluid/gas}}) = 0, \tag{4.2}$$

4.3.1. The heat exchanger

The two heat exchangers required for inter cooling are modelled as a shell- and tube heat exchangers. Hot helium in the tubes is cooled by cold seawater in the shell. The recuperator is simulated as a PCHE heat exchanger. The exchange of heat is simulated based on the E-NTU method as described earlier in section 3.2.3. The concept of the NTU-method is to define heat transfer as a function of the number of transfer units (NTU). This is a way to define the ease at which heat moves between flows, relative to the ease the flows absorb that heat. Heat capacity of the medium depends on specific heat and mass flow as can be read in section 3.2.3. Effectiveness relations are also listed in appendix B. The simulation calculates both thermal resistance and thermal mass. The material in thermal mass calculation is assumed to be stainless steel considering the comparison made in section 3.2.3.

- Adiabatic.
- Flows are single-phase.
- Heat transfer is of sensible heat.
- Compressibility of the gas is taken into account. Yet, this is limited for helium. (factor 1.0005)

4.3.2. Valves

In high temperature and high pressure gas networks a ball valve is commonly used. This type of valve is durable, versatile and features a quick shutoff capability. The latter is crucial with respect to accurate control. The opening of the ball valve is simulated by controlling the opening area via the equation below:

$$A_{\text{open}} = \sin(\varphi) R_{\text{bore}}^2 \left[\cos^{-1}(\lambda_{\text{bore}}) - \lambda_{\text{bore}}\sqrt{1-\lambda_{\text{bore}}}\right] + R_{\text{port}}^2 \left[\cos^{-1}(\lambda_{\text{port}}) - \lambda_{\text{port}}\sqrt{1-\lambda_{\text{port}}}\right] \tag{4.3}$$

$$\lambda_{\text{bore}} = \frac{R_{\text{bore}}^2 - R_{\text{port}}^2 + l^2}{2R_{\text{bore}}l} \tag{4.4}$$

$$\lambda_{\text{port}} = \frac{R_{\text{port}}^2 - R_{\text{bore}}^2 + l^2}{2R_{\text{port}}l} \tag{4.5}$$

R_{port} and R_{bore} are the radii of the valve port and the ball bore, respectively. I is the displacement of the bore centre from the valve port centre. Phi is the rotation of the ball valve.

Purpose valve	S	S_{open}	unit
Before LPC for throttling	0.0314	0.028	m^2
Valve inventory control	0.0078	0.0063	m^2
Turbine throttle	0.0314	0.0314	m^2

Table 4.3: Valve dimensions

Note that the valve dimensions are in line with the nominal diameter of the piping throughout the system: 20 cm. The opening area was slightly reduced iterative to improve response for controlling it.

Momentum balance
The mass flow through the valve is calculated as follow:

$$\dot{m} = C_d S_{\text{open}} \sqrt{\frac{2\gamma}{\gamma - 1} \rho_{\text{in}} p_{\text{in}} \left(\frac{p_{\text{out}}}{p_{\text{in}}}\right)^{\frac{2}{\gamma}} \left[\frac{1 - \left(\frac{p_{\text{out}}}{p_{\text{in}}}\right)^{\frac{\gamma-1}{\gamma}}}{1 - \left(\frac{S_{\text{open}}}{S}\right)^2 \left(\frac{p_{\text{out}}}{p_{\text{in}}}\right)^{\frac{2}{\gamma}}}\right]} \tag{4.6}$$

S_{open} is the valve opening area. S is the area at inlet and outlet. C_d is the discharge coefficient. γ is the isentropic exponent.

4.3.3. Compressor

To be able to take into account the changes in pressure and temperature inside the compressor, the corrected mass flow is adjusted from the inlet mass flow. The pressure ratio and efficiency at nominal inflow condition (4.06 kg/s helium for 5.5 MWth reactor power in the closed helium Brayton example) is set both- as a point of reference and as a point of maximum efficiency. Isentropic efficiency is assumed 87.5% at nominal condition. Change in rotational speed or mass flow rate through the compressor - away from the nominal inflow condition - will result in a lower isentropic efficiency. The isentropic efficiency, pressure ratio, and corrected mass flow rate are functions of speed and map index. The data between data points for efficiency, pressure ratio and corrected mass flow is linearly interpolated.

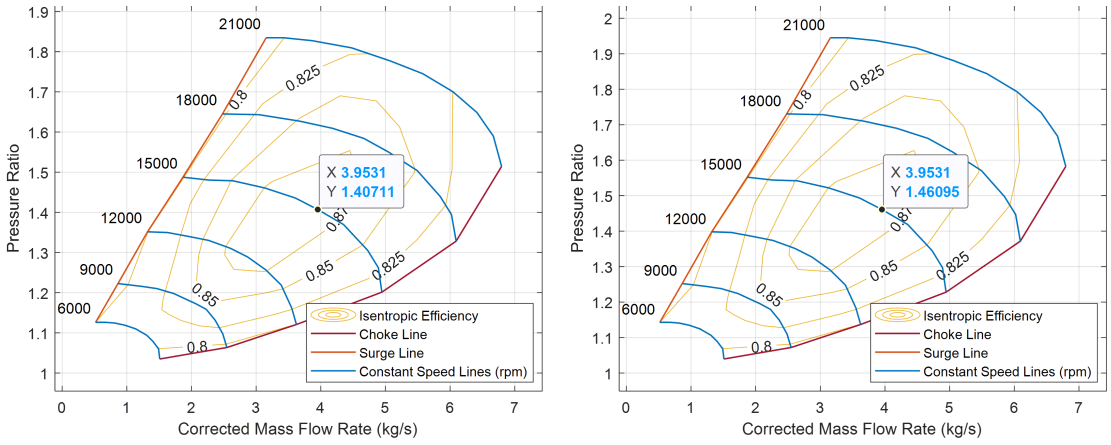

Figure 4.1: View of the LPC and the HPC compressor map - scaled to nominal conditions of the Holos-Quad

$$\dot{m}_{\text{corr}} = \dot{m}_A \left(\sqrt{\frac{T_A}{T_{\text{ref}}}} \Big/ \frac{p_A}{p_{\text{ref}}}\right), \tag{4.7}$$

The shaft speed is also adjusted to the temperature at the inlet of the compressor at nominal conditions (40 degrees Celsius). Mechanical efficiency is assumed to be 98% for both compressors. This could be achieved when using magnetic elevation.

$$\omega_{\text{corr}} = \frac{\omega}{\sqrt{\frac{T_A}{T_{\text{ref}}}}}, \tag{4.8}$$

$$\tau = \frac{\dot{m}_A \Delta h_{\text{total}}}{\eta_m * \omega}, \tag{4.9}$$

P_{fluid} is the hydraulic power delivered to the fluid, which is determined from the change in specific enthalpy.

$$\Phi_A + \Phi_B + P_{\text{fluid}} = 0, \tag{4.10}$$

4.3.4. Turbine

Again for the turbine, a nominal pressure ratio and mass flow is set as a reference. Nominal mass flow 4.08 kg/s and nominal pressure ratio 1.9. For the turbine the isentropic efficiency is simulated to be fixed at 90%. Mechanical efficiency at 98%.

$$\omega_{\text{corr}} = \frac{\omega}{\sqrt{\frac{T_A}{T_{\text{ref}}}}}, \tag{4.11}$$

$$\tau = \frac{\eta_m \dot{m}_A \Delta h_{\text{total}}}{\omega}, \tag{4.12}$$

$$\dot{m}_{\text{corr}} = \dot{m}_A \left(\sqrt{\frac{T_A}{T_{\text{ref}}}} / \frac{p_A}{p_{\text{ref}}} \right), \tag{4.13}$$

By considering the corrected mass flow, the simulation takes into account the changes in temperature and pressure inside the turbine against nominal conditions.

4.3.5. Reactor

The model does not include considerations for the reactor kinetics. This is outside the scope of this research. Instead, it will be calculated how much energy is to be supplied to the fuel inside the reactor in order to keep the coolant temperature at the outlet of the reactor constant - for all events and mechanisms discussed in this report. The advantage of regulating thermal power via this approach, is that is essentially calculates the required combined effect of the negative temperature coefficient and other reactor control measures in place, such as the control rods.

By doing so, the actual reactivity control required to enable this change of thermal power could be verified in a follow-up research. For example, with the 6-point reactor kinetics model.

Parameter	Unit	Value
Number of coolant channels	-	382
Inner Radius coolant channels	cm	0.543
Height reactor core	cm	3.8
Velocity coolant	m/s	40

Table 4.4: Parameters reactor core as taken from the Holos-Quad design

For heat transfer the heat exchanger is modelled as a pipe with a heat exchange surface between coolant and graphite equal to the actual reactor. The convective heat transfer equations can be found in appendix A. The energy and mass balance equations are equal to those shown earlier in this section.

Thermal mass of the reactor is estimated at 6264 kJ/kelvin. Calculation is performed based on information from the Holos-Quad design and can be found in appendix A

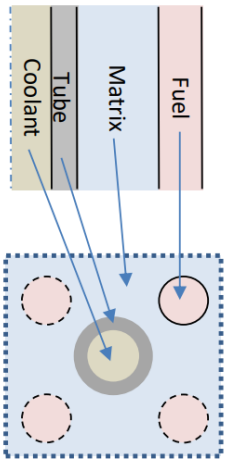

Figure 4.2: Sketch of a coolant-inside-tubes configuration in the reactor [27]

4.3.6. Piping

The pipes are modelled as a constant volume block. The dimensions and volumes are taken from the Holos-Quad design and can be found in appendix A. The same mass- and energy balance equations apply as shown for the reactor above. However, in the pipes there is no convective heat transfer.

4.4. Control mechanisms

The control mechanisms considered and tested in this study are listed in table 4.5. The table contains a brief description of the action + result of the control mechanism. Figure 4.3 contains a sketch of the location of each control mechanism in the cycle.

It can be noted how the turbine bypass is not positioned before the turbine, but before the recuperator. Thus, mass flow to the reactor and turbine is reduced and diverted to pre-cooling instead. This is opted for based on the following arguments. First, to avoid flow disturbance at the most critical point in the cycle - between the turbine and the reactor. This location in the cycle features both the highest pressure and the highest temperature. Thus, a flow disturbance at that point would both impact the reactor and the turbine significantly. When the bypass valve would open before the turbine, the coolant flow through the reactor would increase and cause the reactor to increase power due to the negative temperature coefficient. Also, it could affect aerodynamic stability when not controlled properly. A sudden reduction in mass flow could cause surge to occur. Second, to reduce material-strength complexities. If a closed bypass pipe would suddenly receive a helium flow of 850 degrees Celsius in a matter of seconds, this is not preferable for continuous repeating. Third, when opting to have the bypass in the power cycle, this could potentially be located outside the reactor compartment which brings great advantage on-board of a TSHD from a maintenance point of view .

Having the 'Turbine bypass' before the recuperator is applied in other type of HTGRs as well. Such as the GTHTR-300C and Mi-HTR [30].

Nr.	Control mechanism	Abbreviation	Action	Result
1	Cooling capacity control	CC	Vary cooling flow rate	Energy is dissipated from the system and not used for power generation
2	Reactor control	RC	Adjust reactor power	Enthalpy change of the coolant
3	Bypass control	BC	Divert flow around the turbine, which is to be cooled away	Reduce turbine work
4	Compressor throttle control	CTC	Vary valve opening before LPC	Varying flow rate through compressor
5	Turbine throttle control	TTC	Vary valve opening before turbine	Impact turbine work, impact pressure resistance, impact work by compressors
6	Inventory control	INVC	Add or remove mass of working fluid to the cycle	Chang in density, pressure, and (volume) flow rate of the gas
7	Compressor speed control	CSC	Electronically control speed of the compressors via an independent shaft	Change in coolant mass flow,

Table 4.5: Principle of the different control mechanisms considered

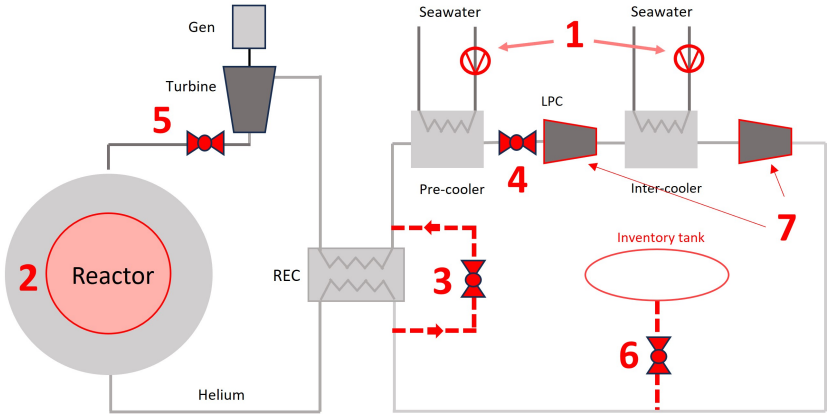

Figure 4.3: A sketch of the locations of each control mechanisms in the power cycle

4.4.1. PI Controller principle

Each control mechanism is simulated via a continuous PI controller. The block output is a weighted sum of the input signal and the integral of the input signal - see equation 4.14 . For each controller the weight of the 'proportional' and 'integral' is manually set to match it function. When applicable, the output of the controller is saturated within set limits and the change rate of the output is limited. The simulation provides feedback of any excessive zero-crossings.

$$u(t) = K_p \cdot e(t) + K_i \cdot \int_0^t e(\tau)\, d\tau \tag{4.14}$$

Next, specific considerations per controller are discussed

4.4.2. Cooling Control (CC)

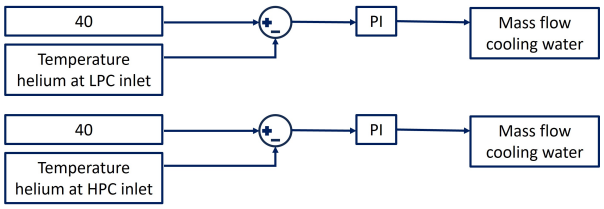

Figure 4.4: PI Cooling capacity control

- Two cooling systems - IC1 and IC2. Both control the inlet temperature of the helium before it enters the LPC or the HPC.
- Set point is 40 degrees Celsius of the helium at inlet of LPC and HPC.
- Inlet temperature of the cooling (sea) water is set at 30 degrees Celsius. Thus, designed for worst conditions given the fact that the temperature of the sea water will be typically be lower - which allows more effective cooling.
- Nominal cooling capacity of each IC is designed to be Ẽ6 kg/s (90 m3/h)
- Heat exchanger designed such that temperature difference of the cooling water from inlet to outside is around 10 degrees Celsius at nominal conditions.

4.4.3. Reactor Control (RC)

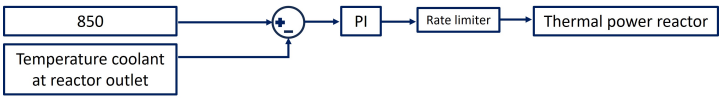

Figure 4.5: PI Reactor Control

- The maximum ramping rate of thermal power by the reactor is limited to 100 % of the maximum reactor power per minute. This was done to limit very excessive oscillations in the system.
- The minimum thermal power of the reactor is limited to 20% of maximum reactor power - as discussed in chapter 3.

4.4.4. Bypass Control (BC)

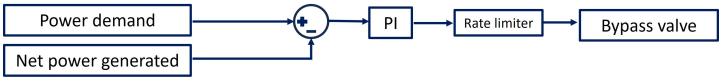

Figure 4.6: PI Bypass control

4.4.5. Compressor Throttle Control (CTC)

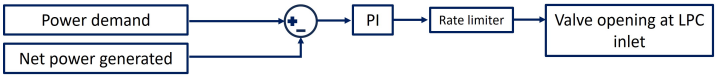

Figure 4.7: PI Compressor Throttling Control

4.4.6. Turbine Throttle Control (TTC)

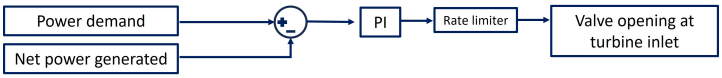

Figure 4.8: PI Turbine throttle control

4.4.7. Inventory Control (INVC)

Figure 4.9: PI Inventory Control

4.4.8. Compressor Speed Control (CSC)

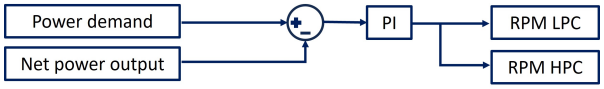

Figure 4.10: PI Compressor speed control

5

The effect of different power control mechanisms

This chapter covers the sub-question:**What is the effect of the different power control mechanisms on the load-following capability of the closed helium Brayton power cycle?**Load following means changing the power generation as closely as possible to the power demand. Both the effectiveness-. and effect on thermodynamic properties in the cycle- is simulated for each control system. The latter refers to sudden changes in temperatures, pressures, flow speeds - amongst other factors - at different locations in the cycle.

5.1. Effect control mechanisms

First, to understand both the effect and the effectiveness of the different control mechanisms on regulating the net power output of the Brayton power cycle, each control mechanisms is assessed individually during a ramp-down. Ramp-down will be referred to as 'Scenario 1'. With respect to operational safety, it is considered that the ramp-down scenario is more crucial than ramp-up. Given the aforementioned - and the limited time available for this research - it is decided to compare the different control systems for this scenario first.

The control mechanisms simulated in this study are:

1. Cooling Control (CC)
2. Reactor Control (RC)
3. Bypass Control (BC)
4. Compressor Throttle Control (CTC)
5. Turbine Throttle Control (TTC)
6. Inventory Control (INVC)
7. Compressor Speed Control (CSC)

There are two control mechanisms always turned on. This is the Reactor Control (RC) and the Cooling Control (CC).

5.2. Scenario 1 - Power demand decreases 10% per minute

For scenario 1, a linear decrease in power demand at 10% of the max power per minute is simulated. Starting at t=120 seconds and ending at 720 seconds when the power demand has decreased to 0% of the max net electric output of the cycle. The 10 % ramp-down scenario was chosen in correspondence to max rates discussed in subsection chapter 3.

To assess the effectiveness and effect, each mechanism is first evaluated on the following aspects:

1. Load following capability. Essentially the difference between load demand and net electric power available.
2. Effect on temperature- and pressure levels, and change rates in the cycle and around the reactor.
3. Effect on surge margin in the compressors.

It can be noted that some starting points show a small deviation. First, because each control mechanism has a different working principle - the nominal condition might differ slightly. Second, for some (valve) controls it was decided to slightly close the valve before performing load-following in order to improve responsiveness. For example, for turbine throttling, the valve opening was reduced to 90% of full opening before initiating the load following scenario. This reduces the mass flow, which requires a larger temperature difference over the reactor, which explains the lower reactor inlet temperature.

Figure 5.1.A shows how each control mechanism was successfully simulated to match the reducing power demand in this scenario.

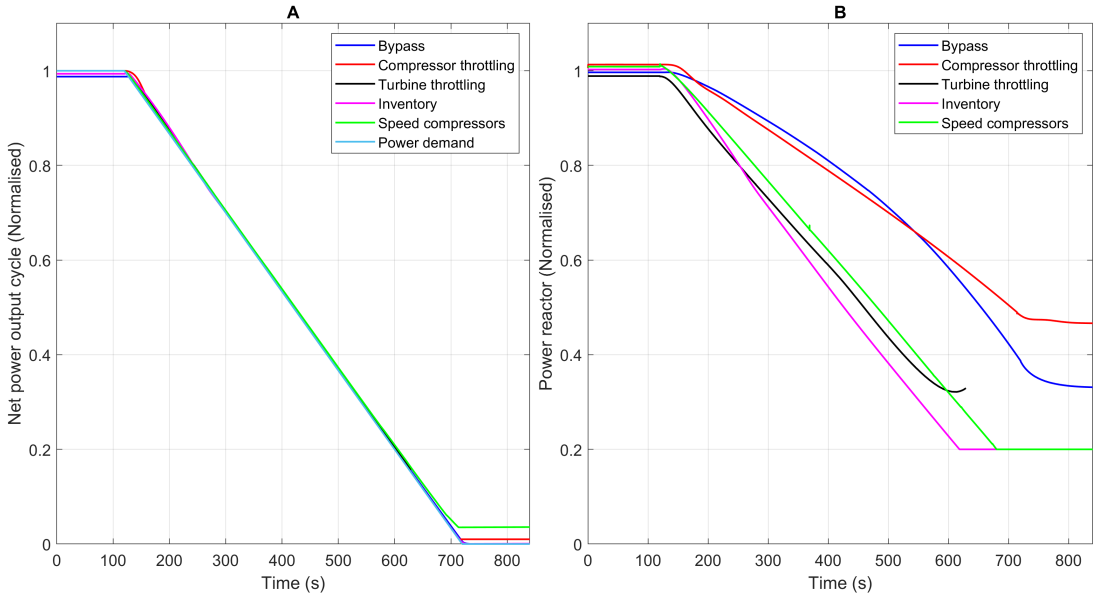

Figure 5.1: A) Load-following for the different control mechanisms. B) Required reactor ramp-down for a constant 10% per minute decrease in power demand.

However, despite adequate load-following for each control mechanism, the underlying thermodynamic effect on the cycle differs. In general, the required reactor power ramping depends on the cycle efficiency and the thermal mass of the reactor. Because when the efficiency of the cycle is reduced, the reactor power reduction could be less for the same net power output. This also holds for cooling. When the heat flux to the coolers is increased, the total cycle efficiency reduces.

Figure 5.1.B shows the required change in reactor thermal power during the transient for the different control mechanisms. Compressor speed control and inventory control both require the reactor to change its thermal power to 20% of max thermal power which was the minimum set-point in the simulation - as explained in Chapter 3. Yet, compressor speed control allows the reactor to ramp down at a slightly lower rate. The cycle efficiency during compressor speed reduction decreases faster compared to inventory control. This explains the small difference. To make this more clear, the efficiencies during ramp down are shown in figure 5.2. In this figure 'Cycle efficiency' refers to: P generated - P HPC -P LPC / P Reactor. Yet, this gives a solid approximation because the power of the water pumps is small relative to the MW-level of the compressors and turbine(s).

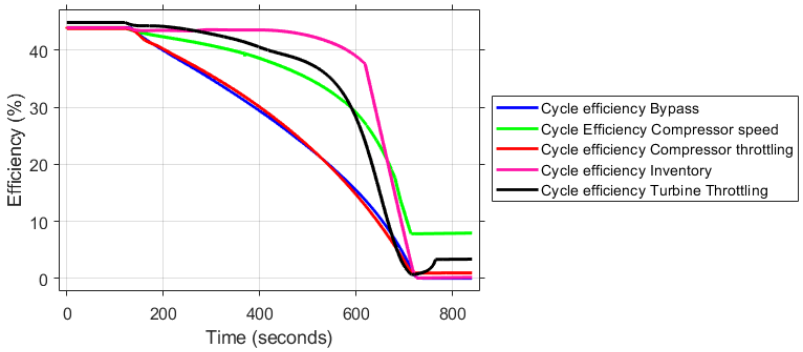

Figure 5.2: Cycle efficiency for the different control mechanisms during scenario 1

While for compressor throttling and bypass control the net power output is successfully lowered to 0% as well, the reactor thermal power would only have to decrease to 47% and 34% of its nominal power respectively. Thus, allowing the reactor to ramp down at a lower rate.

For turbine throttling the plot is cut off at 630 seconds. This was done because at this point the helium mass flow was too low to allow for effective convective heat transfer in the recuperator. This lead to a strong decrease in temperature of the flow going from the recuperator to the reactor which subsequently triggered the reactor to start ramping up again due to the negative temperature coefficient.

Given the high mass flows, a transient power scenario causes significant changes in heat flux throughout the power cycle. Therefore, it is crucial to understand whether the reactor was capable of changing it thermal power output accordingly. Figure 5.3.A shows the temperature change rates at the reactor outlet. The reactor power is controlled by monitoring the coolant temperature at the reactor outlet. Thus, monitoring this gives insight in whether the reactor thermal power could successfully be regulated or not. The figure shows that in the first 80% power reduction (from 120s - 600s), the reactor could successfully adjust its power output. In the last 20%, the temperature at the outlet start increasing for only compressor speed control and inventory control. This is a result from the minimum reactor output of 20%, which was discussed in Chapter 3 and which can also be found in figure 5.1.B.

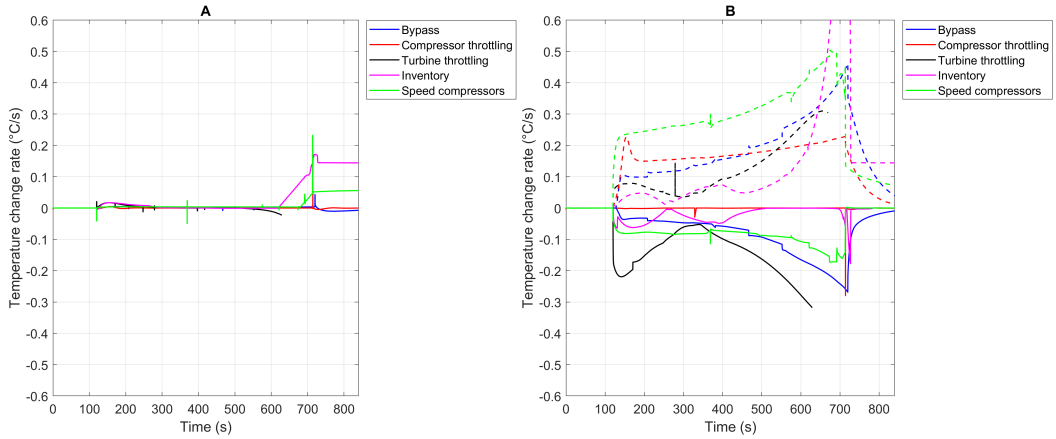

Figure 5.3: A.) Temperature change rate at outlet reactor during decreasing power demand B.) The maximum upward- and downward temperature change rate during decreasing power demand

The temperature change rate of the coolant is measured at any other point in the power cycle as well. From a material point of view it is preferred to minimise temperature change rates. Additionally, it could impact performance of turbomachinery. Therefore, it is relevant to compare the differences in temperature change rates caused by the different control mechanism. Figure 5.3B. shows both the maximum negative- and the maximum positive temperature change rate for each time step at any node

in the total power cycle. It hows how each control mechanism causes thermal gradients in the cycle at any time.

It can be noted how removing helium from the cycle - via inventory control - actually enables very limited temperature fluctuations in the beginning. However, after the power is reduced to 20% - the temperature rises significantly. This is because the reactor remains operating at 20% power.

Controlling the power via compressor speed also induces high temperature change rates. The reduction in mass flow is faster compared to the other controls - as will be shown in 5.6 - and convective heat exchange is reduced.
Compressor throttling and turbine bypass show medium temperature change rates throughout the cycle.
Yet, each control mechanism causes temperature fluctuations exceeding 0.3 degrees Celsius per second after reaching the 20 % power point.

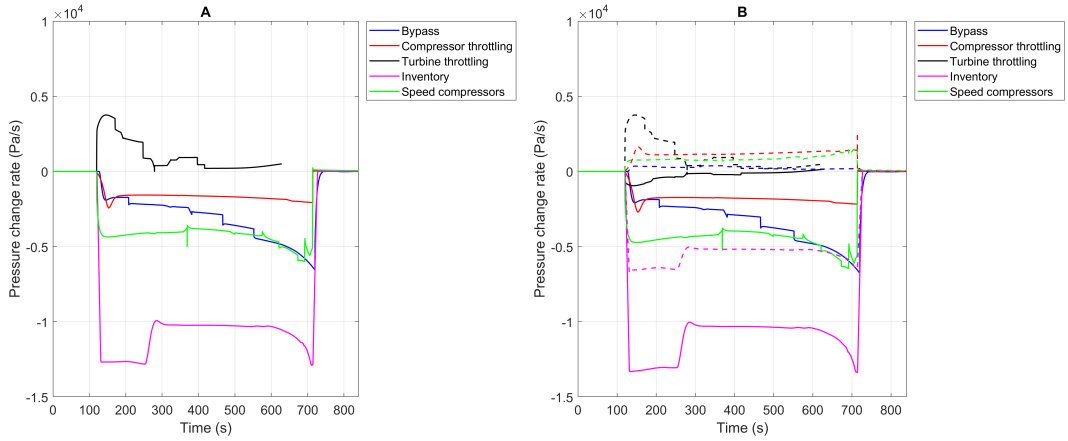

Figure 5.4: A.) Pressure change rate at outlet reactor during decreasing power demand B.) The maximum upward- and downward pressure change rate during decreasing power demand

In addition to temperature, the pressure of the coolant influences the heat flux in the cycle. Figure 5.4A. shows how inventory control causes the pressure at the reactor outlet to decrease at a constant rate. Turbine throttling causes a positive pressure change rate at the reactor outlet - thus exceeding the 7 MPa. Bypass, Compressor speed and compressor throttling cause a gradual decrease in pressure at the reactor outlet whereby compressor throttling induces the lowest pressure decrease.

Figure 5.4B. shows how the largest pressure change rates do actually occur at the reactor outlet. This is because the density of helium is higher at high pressure and temperature, so removing a given mass of helium has a greater effect on the pressure in this region. Consequently, the relative pressure drop will be more pronounced in the high-pressure section of the cycle.

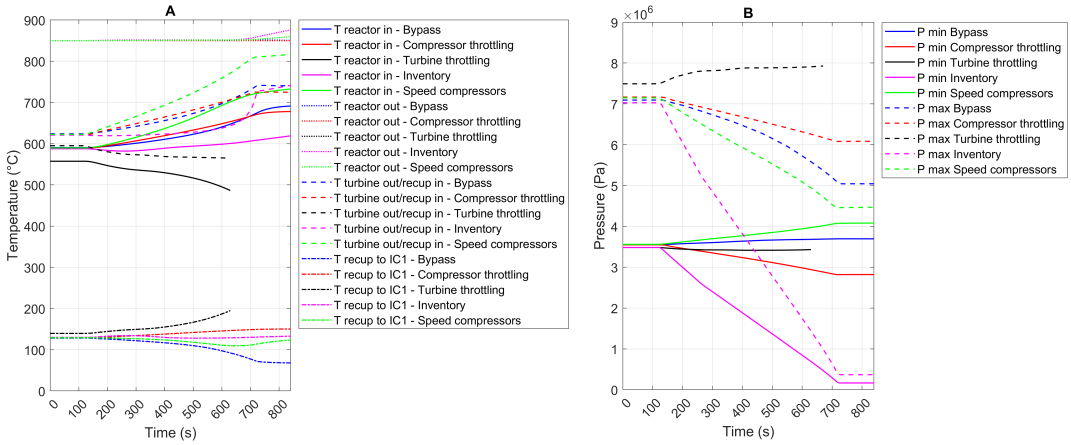

Figure 5.5: A) Temperature levels during decreasing power demand at different positions in closed helium cycle B) Minimum and maximum pressure level in the cycle

Figure 5.5.A shows the temperature at four relevant locations in the recuperated Brayton cycle. Change in temperature of the coolant around the reactor and recuperator impacts reactivity and material strength - amongst other factors - and should therefore be monitored. Due to the negative temperature coefficient, the reactor's power output decreases as the temperature of the coolant increases and vice-versa. Thus, an increase or decrease in coolant temperature will effect the thermal power of the reactor, which is calculated as a required change in thermal power in this model.

First, at the reactor inlet; compressor speed causes a significant temperature rise while the turbine throttling causes a temperature drop. This is because the pressure with turbine throttling remains high. Bypass control and compressor throttling control causes a small increase in temperature. Inventory control shows to have least effect on the temperature level at the inlet of the reactor.

Second, from turbine to recuperator inlet; when the pressure ratio over the turbine reduces the temperature after the turbine increases. Especially, compressor throttling induces a large increase in temperature from the turbine into the recuperator which subsequently increases the temperature of the gas at the reactor inlet.

Figure 5.5.B depicts the minimum- and maximum pressure level in the cycle during scenario 1. The figure shows clearly how turbine throttling causes the maximum pressure in the cycle to exceed 80 bar. Next, it clearly shows the effect of inventory control. By removing coolant mass from the system, the pressure decreases. For helium - as an ideal gas - the change in density, pressure and flow rate is very close to linear with mass reduction, meaning temperatures tend to remain constant.

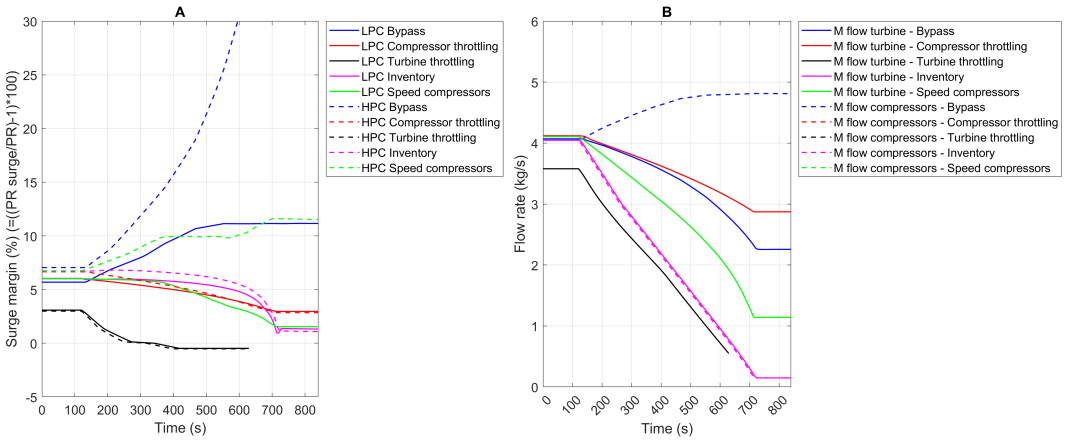

Figure 5.6: A) The surge margin B) The mass flow rate through the compressors and through the turbine

Figure 5.6.A shows the surge margin in the LPC and the HPC during the changing power demand for the different controls. The surge margin is one way to depict the pressure ratio at a given time relative to the pressure ratio at which surge would occur. Except for speed control, the rotational speed of the compressors is kept constant in this simulation. Hence, the surge pressure ratio is found by following the constant speed line - as drawn in figures 4.1 and 4.1.

A negative surge margin indicates surge. When the surge margin increases greatly with respect to nominal conditions, choke could occurs. Although, helium has chock limits at very high relative mass flows as explained earlier in 3.Exact choke and surge limits are to be found via extensive testing experiments. However, figure 5.6 gives insight in how the operational points shifts away from its nominal point - as drawn before in figure 4.1 and 4.1.

Figure 5.6.A shows how turbine throttling causes both the LPC and HPC to pass the surge line when speed is not changed. In contrary, the reduced pressure ratio in the HPC during turbine bypass causes the surge margin to increase significantly. Compressor speed control increases the HPC surge margin slightly and reduces the margin for LPC. Both compressor throttling and inventory control have moderate impact on the surge margin - thus causing fewer aerodynamic instability.

Figure 5.6.B shows how each control mechanism changes the mass flow rate through the cycle. The bypass flow causes the mass flow through the compressors to increase. Inventory control and turbine throttling control cause the mass flow to reduce most significantly.

5.3. Choosing a control mechanism

Given the complexity of combining all control mechanisms simultaneously, it is decided to pick the most suitable and use these to simulate subsequent scenario's. In an attempt to choose the two 'best performing' control mechanisms, a comparison is shown in table 5.1. For each characteristic, the control mechanisms is graded from '- -' to '++'. A '- -' rating is worst and '++' is best. The criteria for comparison have been chosen in accordance to performance parameters and thermodynamic challenges discussed earlier in chapter 3. The table does not contain a weighted score and the comparison is set-up for indicative purpose only.

Control mechanism	Abbrev.	Load-following	Required reactor ramping	Temperature change rate reactor inlet	Max temperature change rate cycle	Pressure change rate reactor	Max pressure change rate cycle	Surge margin compressors
Bypass Control	(BC)	++	++	+/-	+/-	+/-	+/-	++
Compressor Throttle Control	(CTC)	++	++	+/-	+/-	+/-	+/-	+-
Turbine Throttle Control	(TTC)	-	-	- -	-	-	-	- -
Inventory Control	(INVC)	++	-	++	++	- -	- -	-
Compressor Speed Control	(CSC)	++	-	-	-	-	+/-	+/ -

Table 5.1: Comparison of the control mechanism

Table 5.1 shows how turbine throttling performs worst. It causes the pressure and temperature to rise at the point in the cycle where this is already highest. Also, surge could occur and it requires the reactor to ramp at the same rate as the reduction in power demand. Bypass control and compressor throttle control perform best whereby compressor throttling control has a lower effect on the pressure change rate throughout the cycle. Although the indirect effects of the pressure change rates have not been elaborated on, it could induce larger aerodynamic instabilities to the turbomachinery. The advantage of inventory control is the low effect on temperature change rates. This is because the working principle lies in reducing the mass in the system. For helium - as an ideal gas - the change in density, pressure and flow rate is very close to linear with mass reduction, meaning temperatures tend to remain constant. However, it also requires the reactor to ramp down at the same level as the power demand. Lastly, compressor speed control also requires the reactor to ramp down at the same rate and induces large temperature- and pressure change rates both in the system and at the reactor inlet. The effect on surge margin is moderate.

5.3.1. Reflection and validation of results

First, the results are reflected upon. The torque of the turbine is calculated with a constant isentropic efficiency of 0.9 and a constant mechanical efficiency of 0.98. The speed of the turbines remained constant. Therefore, the power of the turbine is directly linear to the product of the mass flow and the total change in the helium specific enthalpy. In a real scenario, scenario 1 would cause the efficiency to change. Also, it would require to adjust the speed of the turbine. Considering the aforementioned, a real life scenario 1 would show a less linear power curve.

Second, in contrary to the turbine, the compressors were simulated with isentropic efficiency lines in the compressor maps. However, these lines are simulated indicatively and could not be validated with actual helium compressor maps. The same holds with the surge line. The results of this simulation show great insight in the shifting of the operational line within the compressor map. Yet, the exact location of the surge line is dependent on actual compressor design and might differ from the surge line assumed in this simulation.

Third, it is expected that the actual reactor kinetics will feature an even faster response to a changing heat flux, compared to the controller in this simulation. This could be advantageous as the peak level of the change rate could possibly be reduced. In contrary, the negative temperature coefficient cannot be controlled and therefore, the reactor should always have sufficient reserve capacity to counteract on the negative temperature coefficient induced in unexpected scenarios. The nuclear physics behind this matter are an essential step in verifying the results.

Next, it would be relevant to validate the performance of the control mechanisms with other studies about the same cycle. There was a study performed about the load following characteristic of the Holos-Quad reactor by Argonne National Laboratory in 2022. The study performed a thermodynamic analysis of a 10% power down scenario as well.

Figure 5.9 shows the required reactor ramping in both studies for a 10% reduction in power demand. Figure 5.12 shows the cycle efficiency during the 10% power reduction in both studies. It is noteworthy to mention that the figures from Argonne National Laboratory show the net generated output on the x-axis instead of the time. However, their simulation also represents a 10% minute ramp-down scenario. It stands out how - except for turbine throttling - the results presented in this report show close proximity to the results presented by Argonne National Laboratory [27]. Argonne National Laboratory is a high rank laboratory in Chicago. This provides some confidence to the validity of the results presented in this report.

However, there are some differences to observe.
First, the results presented in this report showed that the turbine throttling keeps a high level of efficiency in the cycle at the beginning - as can be seen in figure 5.11. While the results from Argonne National Laboratory (ANL) show that the efficiency starts decreases linearly. This can be explained by figure 5.7, which shows how for the ANL simulation the reactor could ramp-down at a lower rate compared to the simulation in this study, inducing the cycle efficiency to decrease faster. Second, in accordance with the previous point, the results from ANL show that the reactor can ramp down at a lower rate. However, when analysing bypass and throttling, the efficiency actually reduces at nearly the same rate. The likely explanation is that in their system the pressure is sustained at a higher level, sustaining a higher mass flow and thereby enabling a higher reactor thermal power.

Based on the work performed by Argonne National Laboratory, the HTGR could possibly be even more flexible in load following compared to the work presented in this report.

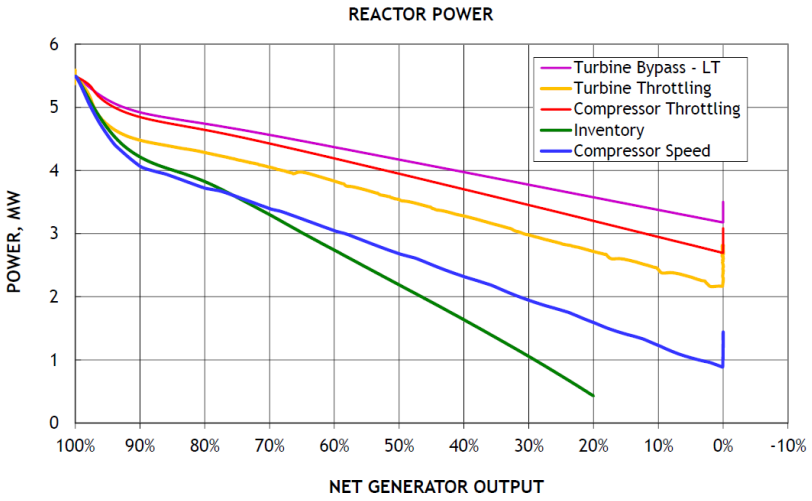

Figure 5.7: Argonne National Laboratory [27]

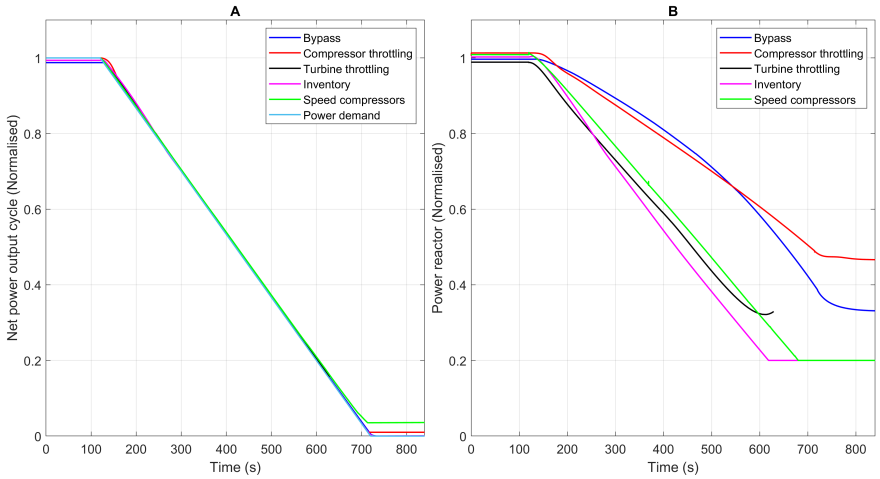

Figure 5.8: Result current study

Figure 5.9: Power overview for a 10%minute load reduction

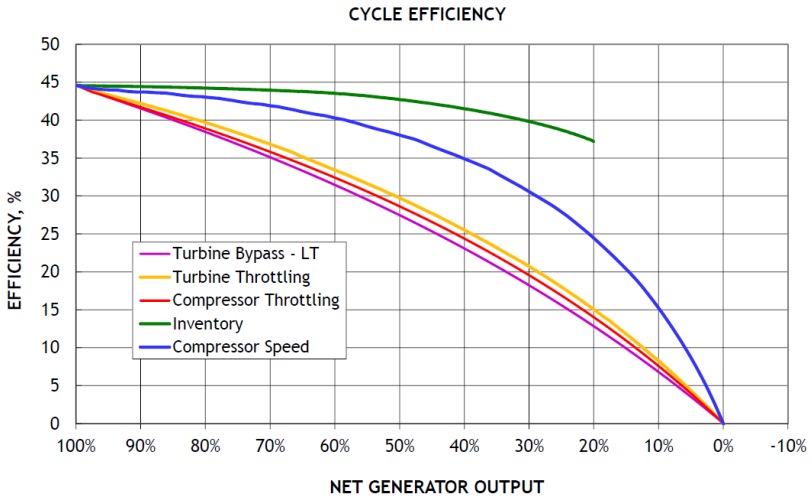

Figure 5.10: Argonne national Laboratory [27]

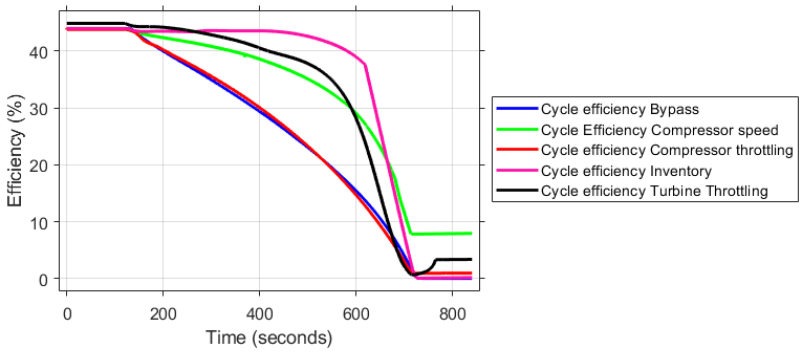

Figure 5.11: Result current study

Figure 5.12: Cycle efficiency for a 10%/minute load reduction

5.4. Chapter conclusion

First, it was found that bypass-, compressor throttle-, compressor speed- and inventory-control, each show the ability to perform the suggested load-following scenario stand-alone. Hereby, bypass control and compressor throttle control even allow the reactor to ramp down at a lower rate than the demand rate, which could be favourable given the purpose of this study.

Second, when looking at temperature change rate in the system, inventory control allows these change rates to be minimum. Bypass and compressor throttling also allow moderate temperature change rates. When assessing the pressure change rates, compressor throttling would induce the lowest pressure gradient. Bypass and compressor speed induce a pressure gradient slightly larger.

Third, the surge margin only changed greatly during bypass and turbine throttling. Turbine throttling could initiate surge to occur in the compressors when the speed is not adjusted. With turbine bypass the surge margin increases towards the choke line. It would be recommended to adjust the speed of the HPC in an extreme transient like scenario 1. Thus, aerodynamic instability could be overcome by adjusting compressor speed accordingly.

All factors considered, it appears that turbine bypass and compressor throttling would be good control mechanisms for more rapid changes in power demand. For slower power transients, inventory control could be a good control mechanisms as this is induces limited temperature change rates throughout the power cycle.

6

Effect load following characteristic HTGR power cycle on powering a TSHD

This chapter should answer the sub-question: **How would the load-following characteristic of the suggested HTGR power cycle effect the operational profile of a TSHD?** First, the challenges for a typical transient load demand of a conventional TSHD are discussed. Second, a load-following scenario is simulated and discussed.

6.1. Challenges transient load demand on board a TSHD

A TSHD-type vessel is known to have different types of operational profiles. These operational profiles - and the transition between these profiles - cause the on-board power demand to fluctuate significantly. The HTGR has its limits when it comes to load-following, as discussed in previous chapters. Therefore, the challenges of the transient load demand on board a TSHD are to be identified.

Figure 6.1A depicts a normalised power overview of a typical dredging cycle for a large TSHD. The dredging cycle is 7.5 hours in this case. The data is taken from an actual TSHD with a total installed power capacity above 25MW. The data is normalised to the cumulative max power installed on-board. To better understand the transients, the activity 'Dredging' can be subdivided in different 'Dredging States'. This example shows the dredging states: Sailing empty, Trailing, Sailing loaded and discharging. Figure 6.1B shows the division of such dredging states over a random period of 24 hours of operations. Figure 6.1C shows the speed over ground during the different dredging states. The figure helps understand the different dredging states.

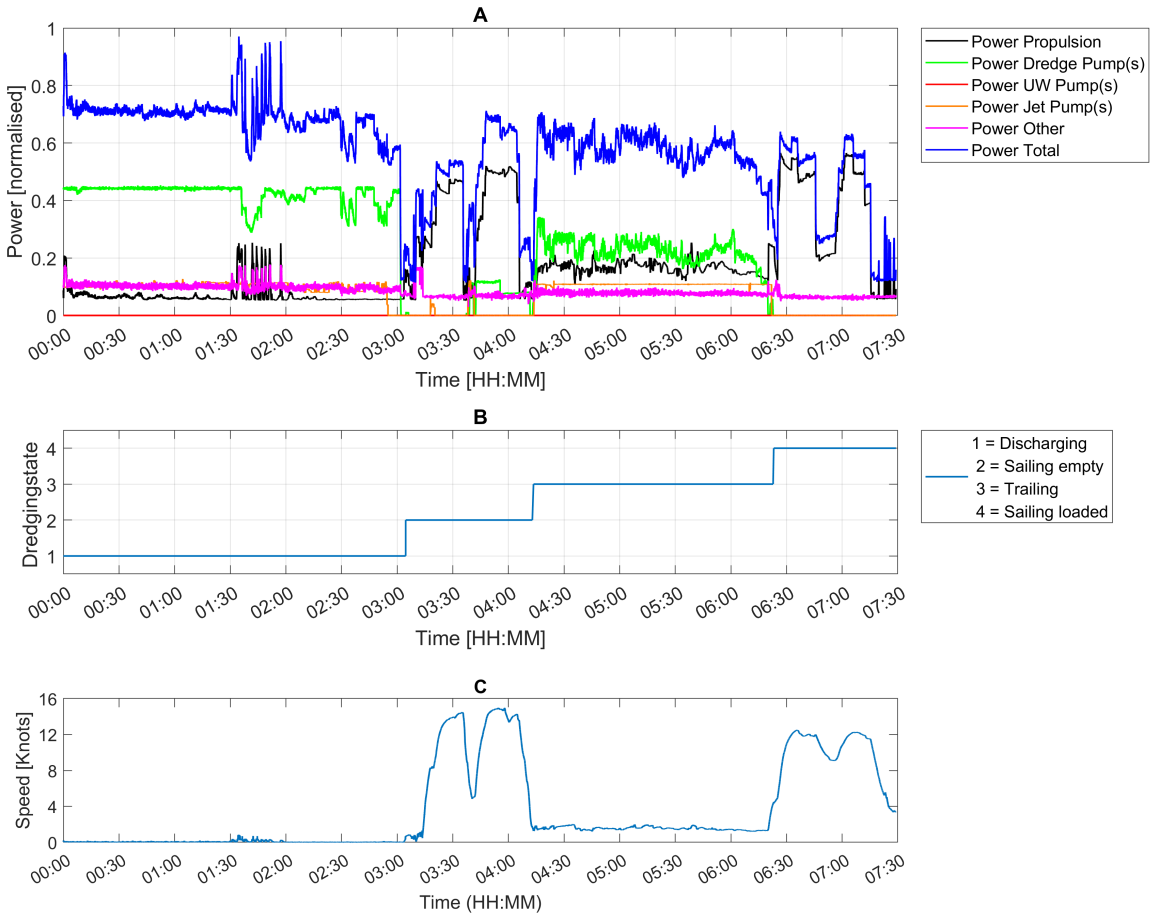

Figure 6.1: A) Power overview typical dredging cycle [normalised] B) Dredging states C) Speed vessel

It can be noted from figure 6.1A that the power demand fluctuates significantly during a period of one dredging cycle. To better understand the transients, the dredging states are plotted separately as well. For each state of dredging, a random period of 30 minutes was picked, see figure 6.2 - 6.5.

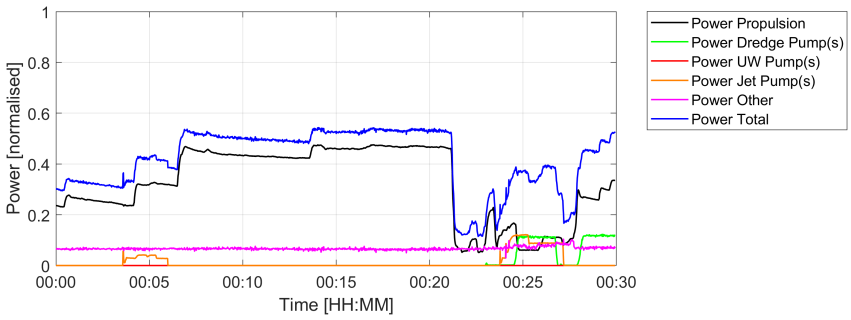

Figure 6.2: Indicative 30 minute power profile: 'Sailing Empty'

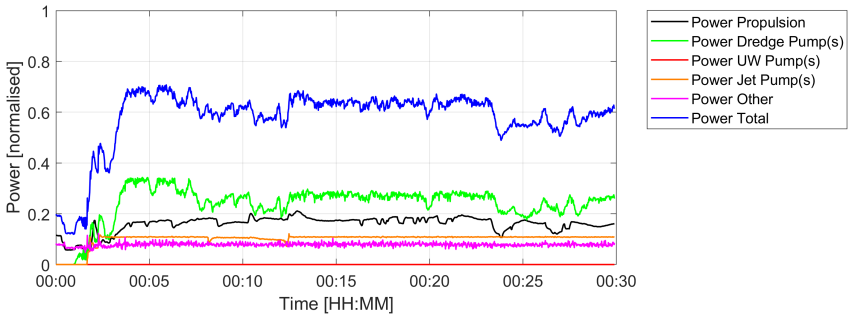

Figure 6.3: Indicative 30 minute power profile: 'Trailing'

When the vessel is trailing or discharging, the vessel uses extra power due to the pumps. Based on the suggested dredging cycle, the activity 'discharging' shows both the highest power peaks and the highest power change rates. The total power demand shifts at rates beyond 60% (of total installed power) per minute as can be seen in figure 6.5

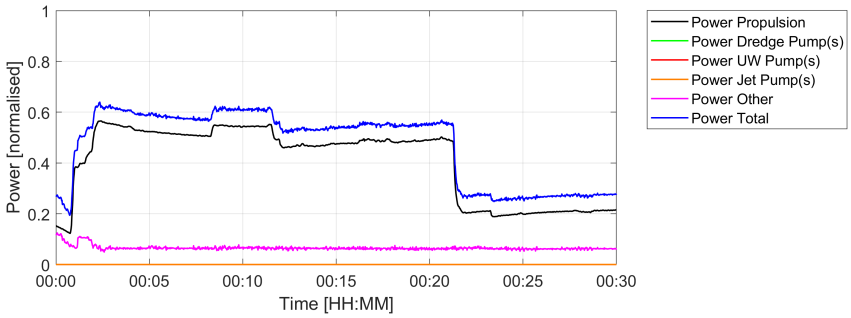

Figure 6.4: Indicative 30 minute power profile: 'Sailing Loaded'

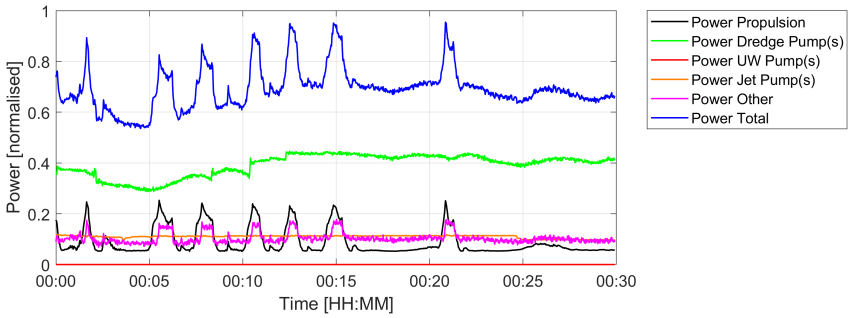

Figure 6.5: Indicative 30 minute power profile: 'Discharging'

Thus, this section showed that the operational profile of a TSHD causes a fluctuating on-board power demand.

6.2. Simulate load-following performance

It is relevant to understand to what extend the suggested HTGR power cycle - as discussed in this research - could match the transient load characteristic of an ICE-powered TSHD today. Therefore, the HTGR is simulated to perform load-following on the varying power demand of a ICE-Powered TSHD, as shown in previous section. By doing so, it is possible to determine whether the operational profile would have to change when sailing on nuclear power in the future.

Chapter 5 discussed how control mechanisms can assist in adapting the net power output to match the varying power demand. Hereby, changes in mass flow, temperature and pressure of the coolant, are monitored around the inlet- and outlet of the reactor. The changes should be minimised as they influence reactor performance, safety, and structural integrity. In addition to the control mechanisms, the reactor - can change power output as well - as discussed in chapter 4 and 5.

6.2.1. Simulation set-up

Chapter 5 showed how both turbine bypass- and compressor throttling control enable favourable load-following characteristics. For the simulation in this chapter, turbine bypass will be applied. This control method allowed the reactor to ramp down at the lowest rate between 100% and 40% of nominal reactor power with acceptable temperature change rates and an increasing surge margin.

The turbine bypass was tested on the fluctuating power demand of the TSHD. The HTGR will not be able to adapt to the high change rates in power demand - up to 60% of max power per minute as shown in 6.1 - due to limitations discussed in chapter 3. Initialising a steep power ramp would induce significant pressure- and temperature changes while still showing a delay on the transient load demand, due to thermal masses in the system and the reactor. Thus, attempting direct load-following on such transients would cause a continuous delay while inducing constant thermal fluctuations that impact both the cycle and the reactor integrity.

Now, it was to be determined to what extend the cycle could realise successfully load following. To do this, it was found effective to apply a low-pass filter to the incoming power demand. The filter can be adjusted to different time-constants.The effect of a low-pass filter is shown in appendix A. This way, small oscillations will have fewer effect on reactor integrity. Clearly, this counts as a gap between power demand and power availability. It was found that a time-filter of 120 seconds together with a demand ramp-rate saturation of 10% per minute, could avoid unnecessary reactor responses and keep the reactor thermal power change rates within 10%.

The simulation of load-following was performed using the same controller settings as described in 5. The max installed power on-board was normalised to the max net generated power output of the reactor model.

To difference between power demand and net power available at each time-step should be resolved by a different - and more rapid - source of energy. Such as an Energy Storage System - as discussed in chapter 3. This could supply additional power in case required, or store energy in case of a surplus.To both understand the load-following power 'gap' and the role of an ESS in this case, the gap between power demand and net generated power output, will be supplied by an ESS in this study.

Find below a short summary of the simulation approach and assumptions

- Active and adaptive control mechanisms: Reactor power, Bypass control, Cooling rate
- HTGR is simulated to supply electrical power via a generator for the cumulative on-board energy demand.
- Power demand is filtered first using a low-pass filter with time constant 120 seconds and a ramp-rate saturation of 10% .
- The reactor control is not saturated to a max change-rate of thermal power output.

6.2.2. Per dredging state

To show the delay in power output by the power cycle with the on-board power demand it is required to zoom in on the power transients. Figures 6.6 - 6.9 depict a normalised power overview of 30 minutes for each dredging state. Each 30 minutes is picked at random and should be taken as indicative examples only.

For slower transients, the figures show that the reactor can perform decent load-following. However for the more rapid power transients, there is a delay between net generated power output and power demand. Also, the figures show a graph of the required net ramping rate of the reactor thermal power. Figure 6.7 shows a peak of 10 % (of max thermal power) per minute. Ramp-up rates are typically

limited to 5% per minute, as discussed in 3. To prevent this, the PTI by batteries could be increased or one could choose to reduce the ramp-up rate when starting trailing - as in this example.

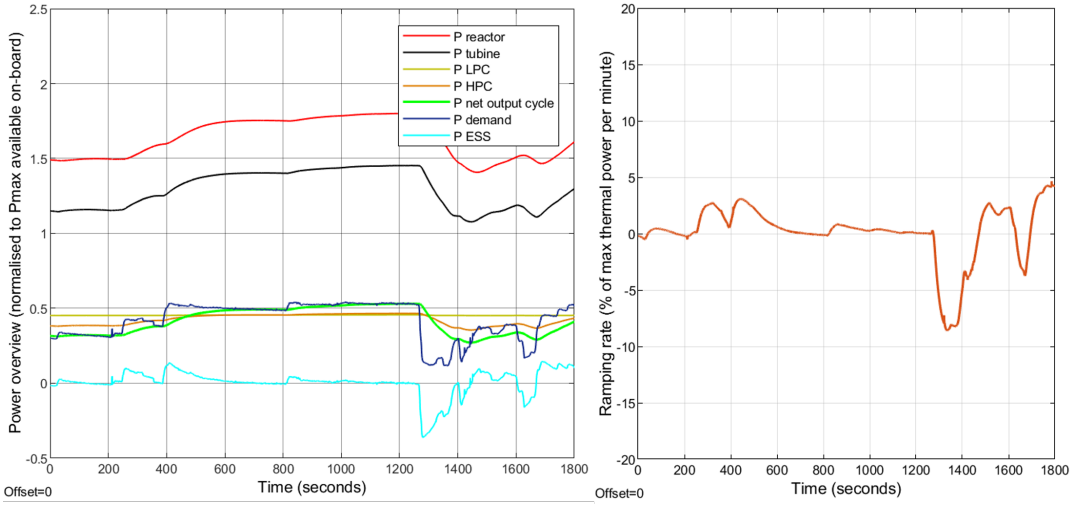

Figure 6.6: Load-following example: 30 minutes sailing empty

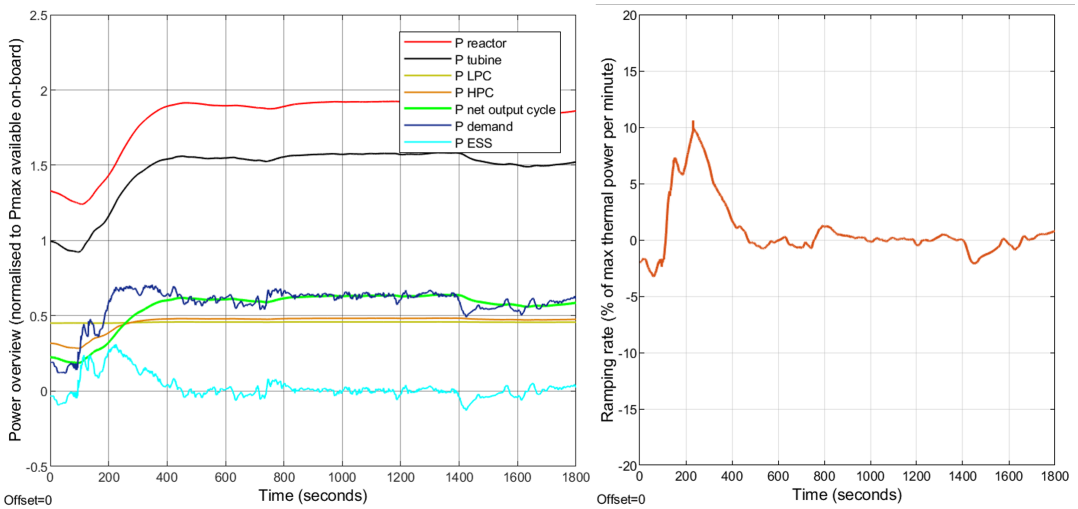

Figure 6.7: Load-following example: 30 minutes trailing

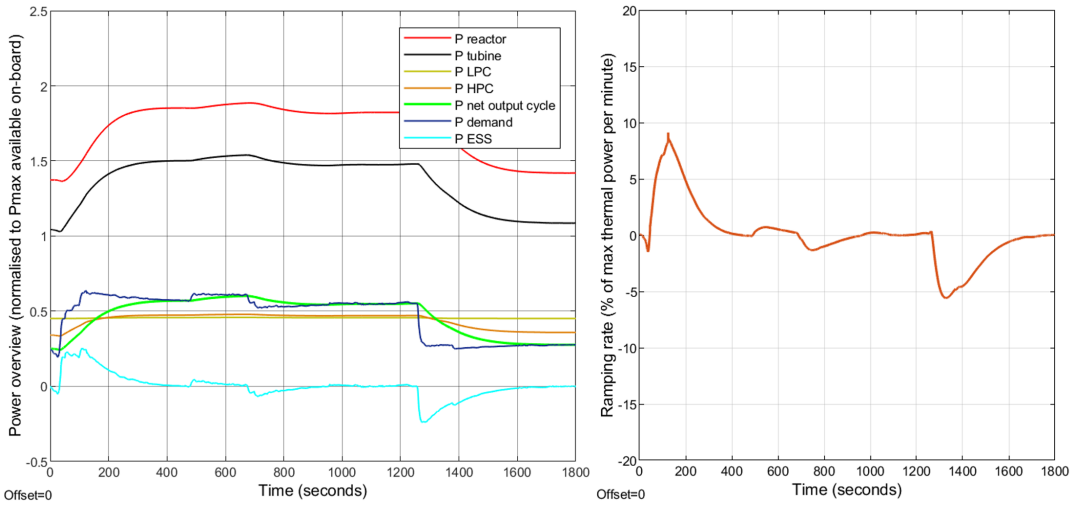

Figure 6.8: Load-following example: 30 minutes sailing loaded

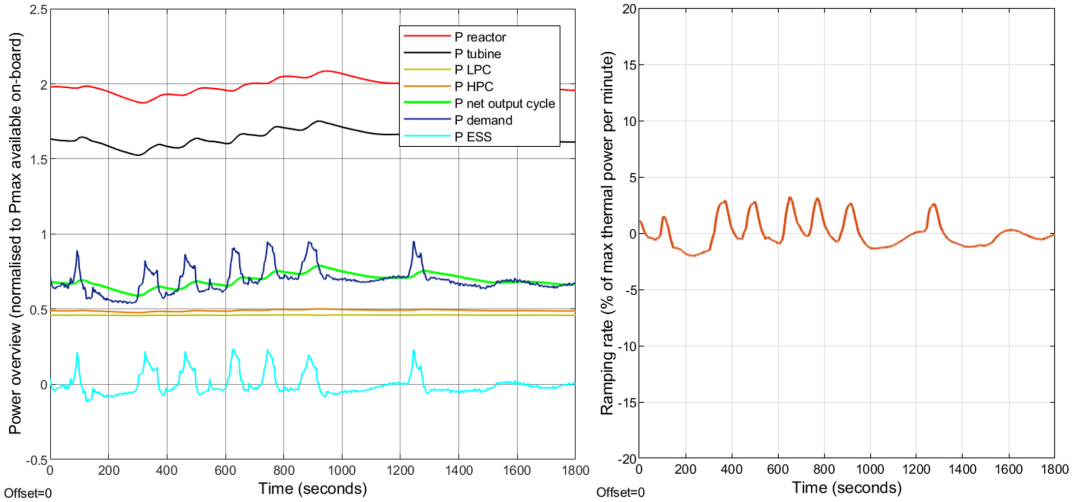

Figure 6.9: Load-following example: 30 minutes discharging

6.3. ESS requirement

To better quantify the mismatch between net generated power and power demand, the role of an ESS is included. Now, the net additional energy requirement can be determined over a certain period.

To provide insight into the size of the ESS requirement, it is decided to scale the normalised values to the power requirement of a typical large TSHD. This will be a TSHD with max 25MWe available on-board. The battery storage capacity is chosen at 3MWh. Assuming a 3C rate and a round trip efficiency of 90%, the battery should be able to supply power up to 8.1 MW. To be able to map the cumulative energy requirement, the ESS is only charged in case of a surplus of power in the power cycle. Shortly summarised below:

- Vessel: 25 MWe TSHD
- Storage capacity battery: 3MWh
- Initial State of Charge (SoC) is 50%
- Round trip efficiency is 90%

6.3.1. ESS requirement for one dredging cycle

Next, the potential role of the ESS is examined for a full dredging cycle. The dredging cycle is 7.5 hours and contains all 4 states as discussed before.

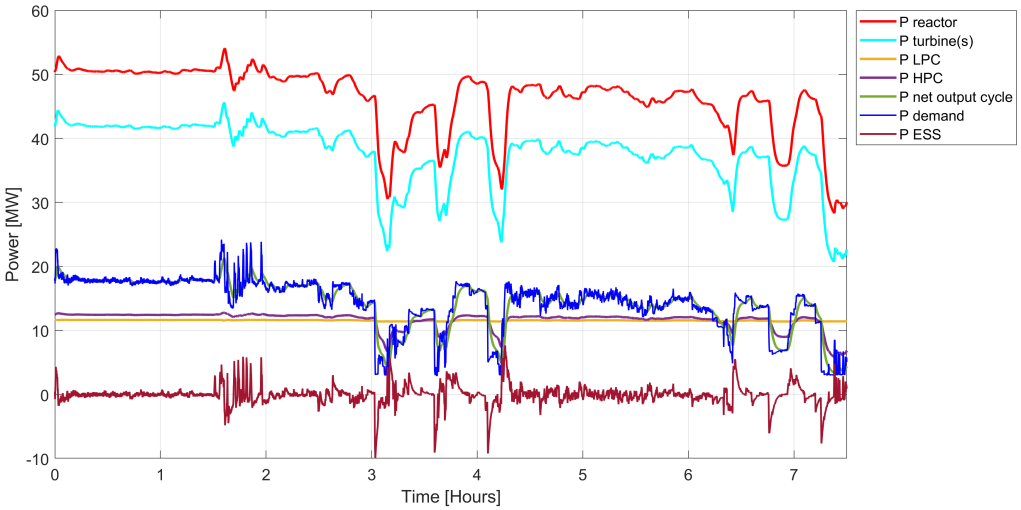

Figure 6.10: One dredging cycle - power overview for a 25 MW TSHD

Figure 6.10 shows how the maximum power requirements by the ESS would actually peak at 10 MW, considering a 25 MW TSHD and given this scenario.

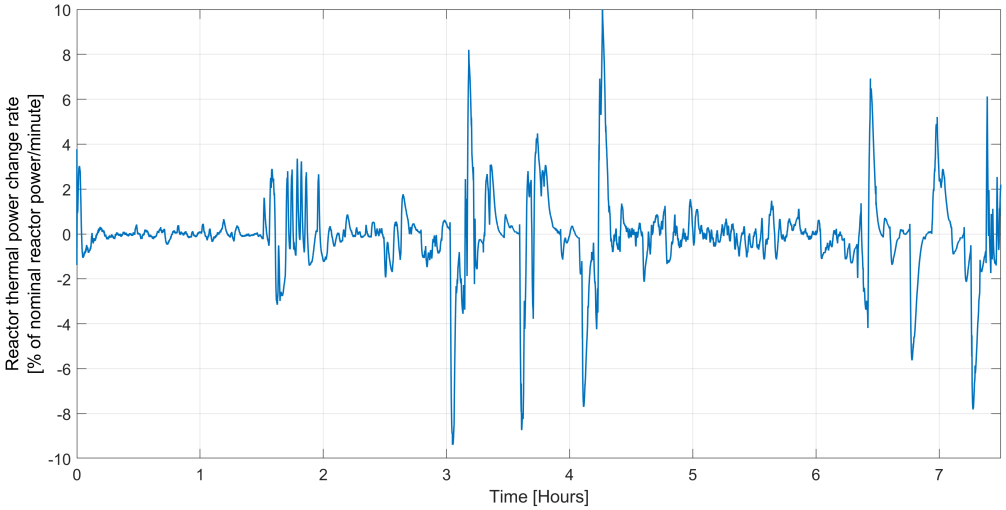

Figure 6.11: Reactor thermal change rate during the 7.5 hours dredging cycle

6.11 shows the required change rate of the reactor thermal power during a full 7.5 dredging cycle. It shows how the reactor thermal power change rate can stay below 10% and that only occasionally peaks of 10% are required.

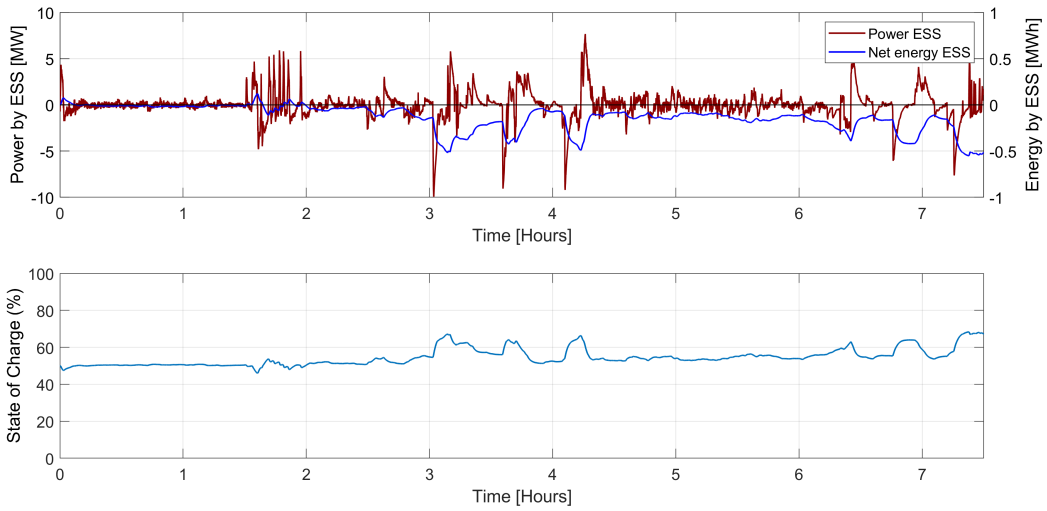

Figure 6.12: Role ESS: Power and state of charge assuming a 3MWh battery pack - for a HTGR-powered 25 MW TSHD

Figure 6.12 depicts the required power take off or power take in by the ESS during the full dredging cycle of 7.5 hours. Also, the state of charge was measured assuming the 3MWh battery pack.

First, it shows how a battery pack of this size would suffice when it comes to the required storage capacity. However, when looking at power, the ESS would have to be charged only a few times at rates a little higher than its power capacity of 8.1 MW. For this situation, it would be advised to reduce the operational demand shifting requirement rather than having to increase the size of the battery pack just to handle a hand-full of power surpluses.

Second, it strikes how the the net energy requirement is relatively stable and cyclical within a 7.5 hours cycle of 4 different dredging states. This turnout favours the application of an ESS.

6.4. Chapter conclusion

This chapter analysed the challenges associated with the transient power demand on board of a typical large TSHD. All dredging states showed significant power fluctuations. Sometimes the cumulative on-board power demand changes beyond 60%/minute.

First, it was shown that the suggested closed helium Brayton cycle cannot perform adequate load-following to the fluctuating demand of a conventional TSHD. The thermal inertia of both the reactor and the system require the thermal power of the reactor to change at high rates. Ineffectively, as the reactor thermal power will oscillate strongly, while still enabling a delay between power demand and power generated.

Second, the feasible limit on load-following was determined. It was found effective to filter the demand in such way that the required change rates of reactor thermal power would not exceed 10%. To quantify the gap between the power demand and the net generated power, the role of the ESS was simulated. For a typical 7.5 hours dredging cycle for a 25 MW TSHD, required discharge power would be up to 8 MW and for charging this would be 10 MW. However, these peaks are only seen a few times in a full 7.5 cycled.

Third, it was shown that the integrated gap between net power generated and power demand is relatively constant - over a full 7.5 hours dredging cycle. This means that the total energy requirement for charging and discharging is relatively close to each other. Therefore, the suggested battery pack of 3MWh for a 25 MW TSHD would be large enough and would have the capacity to perform peak-shaving.

Reflecting on the results, it is important to realise that the thermodynamic characteristic of the cycle is based on a 5.5 MWth reactor and not on a 55 MWTh reactor which would be required on board of a 25 MWe nuclear powered dredging. That having said, it could be possible that the thermal mass of a larger nuclear reactor could be larger or smaller - relatively and thereby showing slightly different results.

7

Conclusion & recommendations

7.1. Conclusion

The main objective of this study was to contribute to establishing the technical feasibility of powering a TSHD by an on-board nuclear reactor in the future. The main research question was:

Could the transient load capabilities of a nuclear-powered TSHD match the dynamic operational power profile of a TSHD?

The secondary research questions in this report should collectively answer this main research question. The results obtained in this study can serve as guidelines for a deeper understanding of the challenges associated with controlling the power output of a (small) high temperature gas reactor. In addition, by simulating the thermodynamics behind a suggested intercooled-recuperated helium Brayton cycle, the purpose of load-following was studied.

Chapter 3 covered the sub-question: **How do the different sub-systems in the closed helium Brayton cycle influence the overall load-following performance of the power cycle?**

The reactor causes a delay in load-following due to its high thermal inertia and the suggested limits on power ramping in order to mitigate impact on material and reactor kinetics. The recuperator should be a compact heat exchanger given the unfavourable heat-capacity ratio and high duty requirement. Larger and less-effective heat exchanger types would induce high thermal inertia and limit the load-following capability of the cycle. The pre-cooler and inter-cooler enable adaption to a changing heat flux before the gas enters the compressor. In the same manner, intercooling enables control of compressor inlet temperature and thereby ensuring both stability and improved performance for the compressors during power transients. Finally, the compressors and turbine(s) play an important role in the overall power cycle as both directly impact the pressure level and flow rates in the power cycle. In transient power scenario's, the turbomachinery should be operated such that high efficiency is maintained and surge, stall or choke is avoided.

Chapter 5 covered the sub question: **What is the effect of the different power control mechanisms on the load following capability of the closed helium Brayton power cycle?**

Turbine throttling was proven least effective. This control mechanism could enable load-following at power levels higher than approximately 30%. However, at lower power levels it would be ineffective and in conflict with the negative temperature coefficient. The main disadvantage of turbine throttling control is the disturbance of heat flux at the point in the cycle with already the highest temperature and pressure level - between the reactor and the turbine. This caused both the max pressure level to surpass 8 MPa and the temperature change rate to exceed 0.3 $^{\circ}$C/s. Finally, the compressors could experience surge when the compressor speed is not adjusted accordingly.

Inventory control has potential to be applied for slower and smaller power transients. The mechanism allows for minimal thermal gradients in the cycle and has little effect on the surge margin of the

compressors. However, individually it can not be effective at lower power levels or in very transient power scenarios.

Bypass-, compressor throttle-, and compressor speed control showed accurate load-following. Of these three, compressor speed induces the highest temperature and pressure gradients, relatively. Which is a disadvantage with respect to structural integrity. Next, bypass- and compressor throttling control could - opposite to compressor speed - enable load-following while allowing the reactor to ramp down at a lower rate, which is considered as a great advantage.

All in all, turbine bypass and compressor throttling would be the best control mechanisms for more rapid changes in power demand. For slower power transients, inventory control could be a good control mechanism.

Chapter 6 covered the sub-question: **How would limitations in load-following effect the operational profile of a HTGR-powered TSHD?**

First, it was shown that the suggested closed helium Brayton cycle cannot perform adequate load following to the fluctuating demand of a conventional TSHD today without an auxiliary source of energy. The thermal inertia of both the reactor and the system would require the reactor to ramp at excessive rates. Ineffectively, as the reactor thermal power is required to oscillate significantly, while still enabling a delay between power demand and power generated.

Second, the power imbalance was analysed while keeping the reactor ramp rates below 10%. For a typical 7.5 hours dredging cycle for a 25 MW TSHD, required discharge power would be up to 8MW and for charging this would be 10 MW. However, these peaks are only seen a few times in a full 7.5 hours dredging cycle. Considering this, accepting a slower operational power shift during those peaks could reduce the required capacity by the ESS.

Third, it was shown that the integrated power imbalance is relatively constant during the suggested 7.5 hours dredging cycle. This means that the total energy requirement for charging and discharging is relatively close to each other. Therefore, the suggested battery pack of 3MWh for a 25 MW TSHD would have be large enough in terms of storage capacity and would have the capacity to perform peak-shaving.

All in all, the limitations in load-following of the suggested HTGR power cycle means that an auxiliary source of power would be required in order to feature the same transient load capabilities as a conventionally powered TSHD. In presence of such auxiliary power source, the operational profile of a TSHD would not be affected.

In conclusion, to address the main research question, a thermodynamic simulation and analysis of a closed helium Brayton cycle demonstrated how control mechanisms can enhance load-following capabilities while minimizing the reactor's ramping requirements. However, the transient load capabilities of the proposed power cycle can only align with the dynamic operational profile of a conventional TSHD if an auxiliary power source is available to manage surplus or deficit power peaks.

7.2. Recommendations

Reactor kinetics
By integrating a reactor kinetics model into the existing framework, the transient load limits of the HTGR can be verified. This should incorporate at minimum: the negative temperature coefficient, neutron life cycle, reactivity control, delayed neutrons, reactor kinetics equations, fuel burnup, and radiation shielding."

Combined effect of the control mechanisms
This research showed the thermodynamic effect of the suggested control systems individually. However, a follow-up study should investigate the combined effect of such control mechanisms as this could potentially increase performance of the cycle and mitigate the thermodynamic- and aerodynamic instabilities. Subsequently, it could improve load-following performance.

Effect of thermal gradients on material
This study showed how a varying load profile induces thermal gradients in the power cycle. Continuous thermal gradients will have an effect on the material properties. Thus, part of assessing the impact of a varying load profile would be to research the impact on the materials. The effect on the material will impact the durability of any sub-system and static element - such as piping. Depending on this effect on material and durability, a different trade-off with respect to load-following could be opted for. In parallel, the effect of repetitive thermal power transients on reactor lifetime should be studied.

More load-following scenario's
Future research should investigate more transient load scenarios to be able to verify whether the suggested HTGR power cycle could match the fluctuating load demand on board of dredging vessels.

More detailed (aerodynamic) analysis of helium turbomachinery
Although the differences between helium turbomachinery and conventional gas turbomachinery have been studied, practical testing of such machinery has been limited to date. As a result, many studies about the rotor-dynamic characteristics of such turbomachinery is yet to be validated. Further research should focus on the aerodynamic implications of helium turbomachinery in combination with the suggested power transients.

The effect of ship motions
The effect of a moving ship on the operation of a high temperature gas reactors should be studied. This is a crucial step before being able to install such reactor on board of a ship.

Redesigning the ship
Assessing technical feasibility would involve studying the conversion from a conventional ship design to a nuclear concept ship design. Insights gained from evaluating the design implications could influence the selection of the preferred power cycle. Besides, the anticipated advantages with nuclear power, such as: higher power at relatively lower OPEX and independence for refuelling, could change design parameters. For example, a higher nominal ship speed or larger dredging equipment.

Regulatory aspect and safety
A critical step toward implementing nuclear-based propulsion on merchant ships in the future is the establishment of a regulatory framework that addresses all related implications. Additionally, the safety aspects of onboard nuclear operations must be thoroughly assessed."

Economical aspect
The development of the high temperature gas reactor is very costly. With PWR type reactors still operating today, there is not much information about the potential costs of high temperature gas reactors and the associated power cycle behind it. The economical aspect should be studied carefully to be able to determine final feasibility of installing such reactor on board of a TSHD.

Public opinion
Lastly, nuclear power could decarbonise - and thereby revolutionise - the maritime industry in the near future. However, whether or not we will power commercial ships with nuclear energy in the future will be determined by politics and public opinion. The challenges and likelihood of overcoming this could be the subject of further study. In the meantime, as engineers, we can do our best to at least ensure technical feasibility.

References

[1] International atomic energy agency. “Small modular reactors for marine-based nuclear power plant”. In: (Nov. 2023). URL: https://aris.iaea.org/Publications/2023%20IAEA%20Marine%20Based%20SMR%20Booklet.pdf.

[2] N. Bartel et al. “Comparative analysis of compact heat exchangers for application as the intermediate heat exchanger for advanced nuclear reactors”. In: *Annals of nuclear energy* 81 (July 2015), pp. 143–149. DOI: 10.1016/j.anucene.2015.03.029. URL: https://www.osti.gov/servlets/purl/1188614.

[3] Xingyan Bian et al. “A comprehensive evaluation of the effect of different control valves on the dynamic performance of a recompression supercritical CO2 Brayton cycle”. In: *Energy* 248 (June 2022), p. 123630. DOI: 10.1016/j.energy.2022.123630. URL: https://doi.org/10.1016/j.energy.2022.123630.

[4] R. J. Brogan. *HEAT EXCHANGERS*. Aug. 2008. DOI: 10.1615/atoz.h.heat\{_}exchangers. URL: https://thermopedia.com/content/832/.

[5] Y.A. Cengel. “Heat and Mass Transfer A Practical Approach 3rd Edition by Cengel20190418 8592 13b2VML”. In: *kmutnb* (Apr. 2019). URL: https://www.academia.edu/38856854/Heat_and_Mass_Transfer_A_Practical_Approach_3rd_Edition_by_Cengel20190418_8592_13b2vml.

[6] Lei Chai and Savvas A. Tassou. “A review of printed circuit heat exchangers for helium and supercritical CO2 Brayton cycles”. In: *Thermal Science and Engineering Progress* 18 (Aug. 2020), p. 100543. DOI: 10.1016/j.tsep.2020.100543. URL: https://doi.org/10.1016/j.tsep.2020.100543.

[7] Choong-Koo Chang and Harold Chisano Oyando. *Load following of small modular reactors*. Sept. 2022. URL: https://encyclopedia.pub/entry/26945.

[8] Sung Wook Choi, In Woo Son, and Jeong Ik Lee. “Comparative Performance Evaluation of Gas Brayton Cycle for Micro–Nuclear Reactors”. In: *Energies* 16.4 (Feb. 2023), p. 2065. DOI: 10.3390/en16042065. URL: https://www.mdpi.com/1996-1073/16/4/2065.

[9] Lindsay Dempsey, Charles W. Forsberg, and Thomas J. Dolan. *Electricity production*. Jan. 2017, pp. 13–28. DOI: 10.1016/b978-0-08-101126-3.00002-6. URL: https://doi.org/10.1016/b978-0-08-101126-3.00002-6.

[10] Vianney Dequiedt et al. *Navigating international taxation: the effects of a carbon levy on shipping*. Tech. rep. 2024. URL: https://ferdi.fr/dl/df-qeuGutDDmWowNYf21YcxT1T7/ferdi-wp340-navigating-international-taxation-the-effects-of-a-carbon-levy.pdf.

[11] Arnold Gad-Briggs. *Analyses of the load following capabilities of Brayton helium gas turbine cycles for Generation IV nuclear power plants*. June 2017. URL: https://dspace.lib.cranfield.ac.uk/handle/1826/12024.

[12] Arnold Gad-Briggs et al. *Closed Brayton-cycle configurations for Gas-cooled Fast Reactors (GFRs) and Very-High-Temperature Reactors (VHTRs)*. Jan. 2023, pp. 777–835. DOI: 10.1016/b978-0-12-820588-4.00029-3. URL: https://www.sciencedirect.com/science/article/pii/B9780128205884000293.

[13] Arnold A. Gad-Briggs et al. *Closed Brayton-cycle configurations for Gas-cooled Fast Reactors (GFRs) and Very-High-Temperature Reactors (VHTRs)*. Jan. 2023, pp. 777–835. DOI: 10.1016/b978-0-12-820588-4.00029-3. URL: https://www.sciencedirect.com/science/article/pii/B9780128205884000293.

[14] Hans David Gougar. *Assessment of the technical maturity of Generation IV concepts for test or demonstration reactor Applications, Revision 2*. 2015. URL: https://inis.iaea.org/search/search.aspx?orig_q=RN:47046053.

[15] Hao Haoran Jr. et al. *Evaluation, comparison and optimization of the compact recuperator for the High Temperature Gas-Cooled Reactor (HTGR) helium turbine system*. Tech. rep., Paper HTR2014-7–1176. URL: https://nucleus.iaea.org/sites/htgr-kb/HTR2014/Paper%20list/Track7/HTR2014-71176.pdf.

[16] Koen Houtkoop. *Nuclear reactors for marine propulsion and power generation systems*. 2022. URL: https://repository.tudelft.nl/islandora/object/uuid%3Afb44c464-6936-4ec6-96b1-52333ff799e3.

[17] Youssef Ismail and Blair Bromley. "ANS 2019 Winter Meeting Presentation: Assessment of Small Modular Reactors (SMRs) for Load-Following..." In: *ResearchGate* (Nov. 2019). URL: https://www.researchgate.net/publication/337548100_ANS_2019_Winter_Meeting_Presentation_Assessment_of_Small_Modular_Reactors_SMRs_for_Load-Following_Capabilities#:~:text=Power%20levels%20for%20SMRs%20can,high%20as%2010%25%2Fmin..

[18] I. Istrate et al. *A review on life cycle assessments of maritime systems combined with an analysis of the THETIS-MRV portal Quantifying Emissions in the European Maritime Sector*. JRC128870. Publications Office of the European Union, 2022. DOI: 10.2760/496363. URL: https://publications.jrc.ec.europa.eu/repository/bitstream/JRC128870/JRC128870_01.pdf.

[19] Peter Jansohn. *Modern gas turbine systems*. Jan. 2013. DOI: 10.1533/9780857096067. URL: https://doi.org/10.1533/9780857096067.

[20] Siddharth Kalra. *Exploratory study on nuclear-powered trailing suction hopper dredgers*. 2020. URL: https://repository.tudelft.nl/islandora/object/uuid%3A73160842-08b7-4c60-a6bd-4a8f53919d63.

[21] L. W. Kays and A. L. London. *Compact Heat Exchangers*. McGraw-Hill, 1955.

[22] In Hun Kim and Hee Cheon No. "Physical model development and optimal design of PCHE for intermediate heat exchangers in HTGRs". In: *Nuclear Engineering and Design* 243 (Feb. 2012), pp. 243–250. DOI: 10.1016/j.nucengdes.2011.11.020. URL: https://doi.org/10.1016/j.nucengdes.2011.11.020.

[23] Zeno Leurs. *Design of a high-speed 20,000 TEU nuclear container vessel*. 2023. URL: https://repository.tudelft.nl/islandora/object/uuid%3Ab15d8ca0-ef54-4801-bc04-64818de3abaf?collection=education.

[24] Sajjad Mahmoudinezhad et al. "A comprehensive review on the current technologies and recent developments in high-temperature heat exchangers". In: *Renewable sustainable energy reviews* 183 (Sept. 2023), p. 113467. DOI: 10.1016/j.rser.2023.113467. URL: https://www.sciencedirect.com/science/article/pii/S1364032123003246.

[25] MatWeb, LLC. *MatWeb Material Property Data*. Accessed: 2024-05-31. 2024. URL: https://www.matweb.com.

[26] Yang Ming et al. "Control strategies and transient characteristics of a 5MWth small modular supercritical CO2 Brayton-cycle reactor system". In: *Applied Thermal Engineering* 235 (Nov. 2023), p. 121302. DOI: 10.1016/j.applthermaleng.2023.121302. URL: https://doi.org/10.1016/j.applthermaleng.2023.121302.

[27] A. Moisseytsev and Claudio Filippone. *Load following analysis of the Holos-Quad 10MWE Micro-Reactor with Plant Dynamics Code*. Tech. rep. May 2022. DOI: 10.2172/1877020. URL: https://doi.org/10.2172/1877020.

[28] NEI. *The nuclear propulsion of merchant ships - Nuclear Engineering International*. Feb. 2024. URL: https://www.neimagazine.com/advanced-reactorsfusion/the-nuclear-propulsion-of-merchant-ships/?cf-view.

[29] Jeremy Henry Owston. "Transient analysis of a direct cycle nuclear heated gas turbine plant with nitrogen coolant". In: *Nuclear Engineering and Design* 397 (Oct. 2022), p. 111928. DOI: 10.1016/j.nucengdes.2022.111928. URL: https://doi.org/10.1016/j.nucengdes.2022.111928.

[30] Leilei Qiu et al. "Dynamic modelling and control system design of micro-high-temperature gas-cooled reactor with helium Brayton cycle". In: *Energy* 278 (Sept. 2023), p. 128030. DOI: 10.1016/j.energy.2023.128030. URL: https://doi.org/10.1016/j.energy.2023.128030.

[31] Ramesh K. Shah and Dušan P. Sekulic. *Fundamentals of heat exchanger Design*. John Wiley Sons, Inc., 2003. URL: https://windyhm.wordpress.com/wp-content/uploads/2008/11/fundamentals-of-heat-exchanger-design-0471321710.pdf.

[32] *Small nuclear power reactors - World Nuclear Association*. URL: https://www.world-nuclear.org/information-library/nuclear-fuel-cycle/nuclear-power-reactors/small-nuclear-power-reactors.aspx.

[33] N. Stauff, C. H. Lee, and C. Filippone. *Core design of the Holos-Quad Microreactor*. Tech. rep. Mar. 2022. DOI: 10.2172/1863405. URL: https://doi.org/10.2172/1863405.

[34] *Supercritical carbon dioxide cycles for Generation IV nuclear reactors*. 2014. URL: http://large.stanford.edu/courses/2014/ph241/dunham1/.

[35] NASA Technology Readiness Assessment (TRA) Study Team et al. *Final report of the NASA Technology Readiness Assessment (TRA) Study Team*. Tech. rep. Mar. 2016. URL: https://ntrs.nasa.gov/api/citations/20170005794/downloads/20170005794.pdf.

[36] B. Thonon et al. "COMPACT HEAT EXCHANGER TECHNOLOGIES FOR THE HTRS RECUPERATOR APPLICATION". In: *COMPACT HEAT EXCHANGER TECHNOLOGIES FOR THE HTRs RECUPERATOR APPLICATION* (). URL: https://inis.iaea.org/collection/NCLCollectionStore/_Public/32/047/32047838.pdf?r=1&r=1.

[37] Zhitao Tian et al. "Axial helium compressor for high-temperature gas-cooled reactor: A review". In: *Annals of Nuclear Energy* 130 (Aug. 2019), pp. 54–68. DOI: 10.1016/j.anucene.2019.02.032. URL: https://doi.org/10.1016/j.anucene.2019.02.032.

[38] Bureau Veritas. "Nuclear in marine". In: 2023.

[39] Jie Wang and Yihua Gu. "Parametric studies on different gas turbine cycles for a high temperature gas-cooled reactor". In: *Nuclear engineering and design* 235.16 (July 2005), pp. 1761–1772. DOI: 10.1016/j.nucengdes.2005.02.007. URL: https://www.sciencedirect.com/science/article/pii/S0029549305000828?ref=pdf_download&fr=RR-2&rr=89cee0272ae90b6c.

[40] Shifa Wu et al. "A load following control strategy for Chinese modular High-Temperature Gas-Cooled reactor HTR-PM". In: *Energy* 263 (Jan. 2023), p. 125459. DOI: 10.1016/j.energy.2022.125459. URL: https://doi.org/10.1016/j.energy.2022.125459.

[41] *XE-100 — High-Temperature Gas Cooled Nuclear Reactors (HTGR) — X-energy*. Apr. 2024. URL: https://x-energy.com/reactors/xe-100.

[42] Gherardo Zambonini. *Unsteady dynamics of corner separation in a linear compressor cascade*. Tech. rep. 2016. URL: https://www.researchgate.net/publication/314290577_Unsteady_dynamics_of_corner_separation_in_a_linear_compressor_cascade.

[43] المصري. محمود "Fluid Mechanics seventh edition by Frank M. White". In: *liu-lb* (May 2018). URL: https://www.academia.edu/36616285/Fluid_Mechanics_seventh_edition_by_Frank_M_White.

A

Model settings Matlab Simulink

A.1. PI Controller settings

Control	Abbrev.	Type	Time domain	Proportional (P)	Integral (I)	Initial condition	Unit	Upper limit	Lower limit	Kb
Cooling 1	CC	PI	Continuous	-5	-0.7	25	kg/s	75	0.125	1
Cooling 2	CC	PI	Continuous	-7	-0.7	25	kg/s	75	0.125	1
Reactor	RC	PI	Continuous	40000	10000	P_Reactor	W	1.01×P_Reactor	0.2×P_Reactor	1
Bypass	BC	PI	Continuous	-0.09	-0.08	0	rad	$\pi/4$	0	1
Compressor Throttle	CTC	PI	Continuous	0.7	0.35	1.49945	rad	1.49945	$\pi/15.3$	1
Turbine Throttle	TTC	PI	Continuous	0.1	0.05	0.9	-	0.9	0.15	1
Inventory	INVC	PI	Continuous	-0.1	-0.03	0	kg/s	0.045	-0.043	1
Compressor speed active load control	CSC	PI	Continuous	30	10	15000	RPM	16000	6000	1
LPC speed regulating	CSC	PI	Continuous	100	20	15000	RPM	16000	6000	1
HPC speed regulating	CSC	PI	Continuous	100	10	15000	RPM	16000	6000	1

Table A.1: PI parameters controllers

A.2. Reactor characteristics

Estimating the thermal mass of the 5.5MWth HTGR 'Holos Quad' concept

	Total volume m3		density kg/m3	kg	Cp J/kg*k	Thermall mass
Volume reactor (m3)	4,928					
Cross section ref. section	63,203	cm^2				
%fuel	20%	0,99	3200	3174,64	400	1269857,0
%coolant	4%	0,22				
%cladding andtube	10%	0,49	3200	1576,97	700	1103881,0
%graphite	65%	3,23	1700	5485,02	710	3894366,4
Average					612,3	
Total				10236,6		6268104,4

Figure A.1: Estimation thermal mass 5.5MWth HTGR

Scale piping from reference reactor to different size on-board reactor

Set power reactor	5,5	MWth
Reference power reactor	5,5	MWth
Scale coefficient	1	-
Reference diameter piping	0,2	meter

*reference reactor: 5.5MWth HTGR Holos Quad

Piping From	To	Mass flow kg/s	Temperature Kelvin	Pressure Pa	M kg/mol	R j/mol*k	Density kg/m3	Thickness wa m	Length m	D_coeff	D_pipe	Area m2	Volume m3	Speed m/s
Recup	IC1	4,08	398	3500000	0,004	8,31	4,23	0,025	0,75	1	0,2	0,0314	0,0236	30,68
IC1	LPC	4,08	313	3500000	0,004	8,31	5,38	0,025	0,5	1	0,2	0,0314	0,0157	24,12
LPC	IC2	4,08	364	4900000	0,004	8,31	6,48	0,025	0,5	1	0,2	0,0314	0,0157	20,04
IC2	HPC	4,08	313	4900000	0,004	8,31	7,54	0,025	0,5	1	0,2	0,0314	0,0157	17,23
HPC	RECUP	4,08	368	7000000	0,004	8,31	9,16	0,025	1,5	1	0,2	0,0314	0,0471	14,18
RECUP	Reactor	4,08	863	6886000	0,004	8,31	3,84	0,025	0,5	0,60	0,12	0,0113	0,0057	93,91
Reactor	Turbine	4,08	1123	6850000	0,004	8,31	2,94	0,025	0,5	0,65	0,13	0,0133	0,0066	104,67
Turbine	Recuperator	4,08	620	3616000	0,004	8,31	2,81	0,025	6	1	0,2	0,0314	0,1885	46,25

Figure A.2: Dimensions of the piping connections between different sub-systems

A.3. Additional equations reactor model

This section shows additional equations used for simulating the heat transfer in the reactor.

First, the partial derivatives of the mass and internal energy of the gas volume, with respect to the pressure and temperature at constant volume. This takes into account the helium gas properties as shown in table 4.2.

$$\frac{\partial M}{\partial p} = V\frac{\rho_I}{p_I} \tag{A.1}$$

$$\frac{\partial M}{\partial T} = -V\frac{\rho_I}{T_I} \tag{A.2}$$

$$\frac{\partial U}{\partial p} = V\left(\frac{h_I}{ZRT_I} - 1\right) \tag{A.3}$$

$$\frac{\partial U}{\partial T} = V\rho_I\left(c_{pI} - \frac{h_I}{T_I}\right) \tag{A.4}$$

- ρ_I: Density of the gas volume.
- V: Volume of the gas.
- h_I: Specific enthalpy of the gas volume.
- Z: Compressibility factor.
- R: Specific gas constant.
- T_I: Temperature of the gas.
- c_{pI}: Specific heat at constant pressure of the gas volume.

Convection Convective heat transfer equation as derived from [5] and [43].

$$Q_H = Q_{conv} + \frac{k_f S_{surf}}{D_h}(T_H - T_I) \tag{A.5}$$

$$Q_{conv} = \dot{m}_{avg}c_{pavg}(T_H - T_{in})\left(1 - \exp\left(-\frac{h_{coeff}S_{surf}}{\dot{m}_{avg}c_{pavg}}\right)\right) \tag{A.6}$$

$$h_{coeff} = \frac{Nuk_{avg}}{D_h} \tag{A.7}$$

$$Nu_{turb} = \frac{\frac{f_{Darcy}}{8}\left(Re_{avg} - 1000\right) Pr_{avg}}{1 + 12.7\left(\frac{f_{Darcy}}{8}\right)^{1/2}\left(Pr_{avg}^{2/3} - 1\right)} \tag{A.8}$$

$$Re_{avg} = \frac{\dot{m}_{avg} D_h}{S_{avg}} \tag{A.9}$$

- Q_H: Total heat transfer rate.
- Q_{conv}: Convective heat transfer rate.
- k_f: Thermal conductivity of the fluid.
- S_{surf}: Surface area of the pipe, $S_{surf} = 4SL/D_h$.
- D_h: Hydraulic diameter of the pipe.
- T_H: High (wall) temperature.
- T_I: Internal gas temperature.
- T_{in}: Inlet temperature (depending on flow direction).
- $\dot{m}_{avg}$: Average mass flow rate.
- c_{pavg}: Average specific heat at constant pressure.
- h_{coeff}: Heat transfer coefficient.
- Nu: Nusselt number.
- k_{avg}: Average thermal conductivity.
- f_{Darcy}: Darcy friction factor.
- Re_{avg}: Average Reynolds number.
- Pr_{avg}: Average Prandtl number.
- S_{avg}: Average surface area.
- Laminar flow for Re < 2000
- Turbulent flow for Re > 4000
- Length flow path = 3.8 meter (height of the reactor)
- For laminar flow Nusselt number is 3.66
- Laminar friction constant for Darcy friction factor = 64
- Internal surface absolute roughness = $15 * 10^{-6}$

A.4. Effect low-pass filter

The figure below shows the effect of a low-pass filter for different time constants. The filter is applied on a randomly picked 6 hour power transient of a large TSHD.

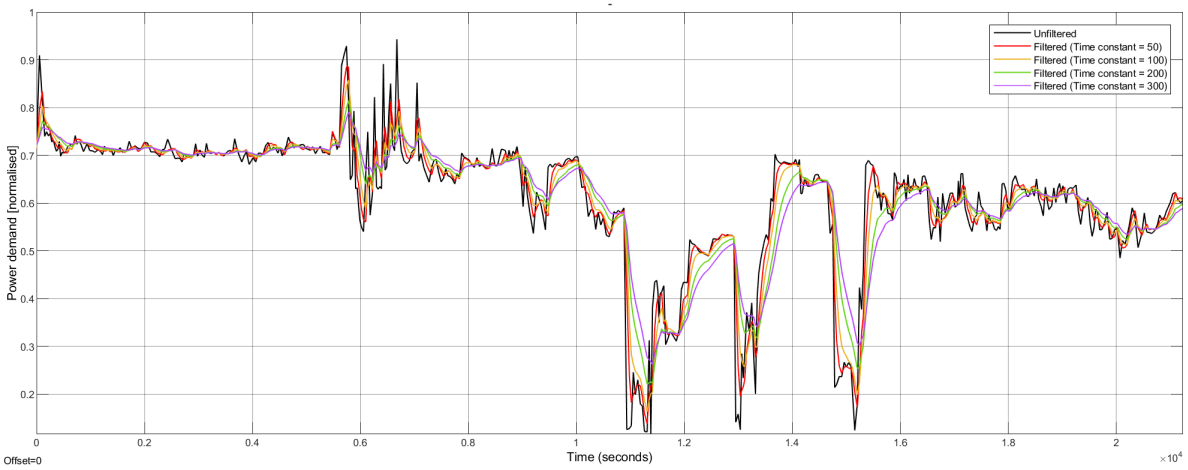

Figure A.3: The effect of applying a low-pass filter on the power demand fluctuations

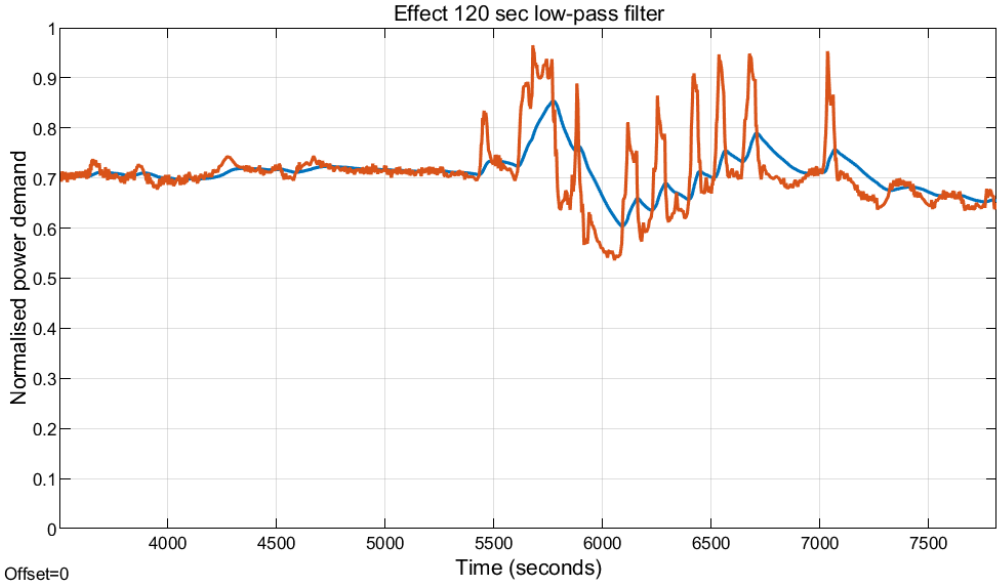

Figure A.4: The effect of a 120 seconds low-pass filter which was used during load following on the TSHD power demand only.

B

Calculations heat exchangers

B.1. Flow arrangement relations

Flow Arrangement	ε-NTU Formulas	ε-NTU Formulas for $C^* = 1$	Asymptotic Value of ε When NTU $\to \infty$
Counterflow	$\varepsilon = \dfrac{1-\exp[-\mathrm{NTU}(1-C^*)]}{1-C^*\exp[-\mathrm{NTU}(1-C^*)]}$	$\varepsilon = \dfrac{\mathrm{NTU}}{1+\mathrm{NTU}}$	$\varepsilon = 1$ fop all C^*
Parallelflow	$\varepsilon = \dfrac{1-\exp[-\mathrm{NTU}(1+C^*)]}{1+C^*}$	$\varepsilon = \frac{1}{2}[1-\exp(-\mathrm{NTU})]$	$\varepsilon = \dfrac{1}{1+C^*}$
Crossflow, both fluids unmixed	$\varepsilon = 1-\exp(-\mathrm{NTU})$ $-\exp[-(1+C^*)\mathrm{NTU}]\sum_{n=1}^{\infty} C^{*n} P_n(\mathrm{NTU})$ $P_n(y) = \dfrac{1}{(n+1)!}\sum_{j=1}^{n} \dfrac{(n+1-j)}{j!} y^{n+j}$	Same as general formula with $C^* = 1$	$\varepsilon = 1$ for all C^*
Crossflow, one fluid mixed, other unmixed	For $C_{\min}$ mixed, $C_{\max}$ unmixed, $\varepsilon = 1-\exp\{-[1-\exp(-\mathrm{NTU}\cdot C^*)]/C^*\}$	$\varepsilon = 1-\exp\{-[1-\exp(-\mathrm{NTU})]\}$	For $C_{\min}$ mixed, $\varepsilon = 1-\exp(-1/C^*)$
	For $C_{\max}$ mixed, $C_{\min}$ unmixed, $\varepsilon = \dfrac{1}{C^*}(1-\exp\{-C^*[1-\exp(-\mathrm{NTU})]\})$	$\varepsilon = 1-\exp\{-[1-\exp(-\mathrm{NTU})]\}$	For $C_{\max}$ mixed, $\varepsilon = [1-\exp(-C^*)]/C^*$
Crossflow, both fluids mixed	$\varepsilon = \dfrac{1}{\dfrac{1}{1-\exp(-\mathrm{NTU})} + \dfrac{C^*}{1-\exp(-\mathrm{NTU}\cdot C^*)} - \dfrac{1}{\mathrm{NTU}}}$	$\varepsilon = \dfrac{1}{2/[1-\exp(-\mathrm{NTU})] - 1/\mathrm{NTU}}$	$\varepsilon = \dfrac{1}{1+C^*}$
1–2 shell-and-tube exchanger; shell fluid mixed; TEMA E shell	$\varepsilon = \dfrac{2}{(1+C^*)+(1+C^{*2})^{1/2}\coth(\Gamma/2)}$ where $\Gamma = \mathrm{NTU}(1+C^{*2})^{1/2}$ $\coth(\Gamma/2) = (1+e^{-\Gamma})/(1-e^{-\Gamma})$	$\varepsilon = \dfrac{2}{2+\sqrt{2}\coth(\Gamma/2)}$ where $\Gamma = \sqrt{2}\,\mathrm{NTU}$	$\varepsilon = \dfrac{2}{(1+C^*)+(1+C^{*2})^{1/2}}$

Figure B.1: $\epsilon - NTU$ formulas and limiting values of ϵ for $C_r = 1$ and $NTU- > \infty$ for various heat exchangers [31]

B.2. Detailed design pre-cooler and inter-cooler used in the simulations

Design characteristics for cooling a 5.5 MWth HTGR
Shell & tube heat exchanger(s) for intercooling with seawater

Liquid flow - Cold		Cooler 1	Cooler 2	
Medium		**Sea_water**	**Sea_water**	
Cp	j/k*kg	3993	3993	
M_flow	kg/s	25	25	
T_cold_1	Celsius	30	30	
T_cold_2	Celsius	42	42	set max cooling outlet
C_cold		99825	99825	
Pressure	bar	1,03	1,03	*averaged*
Density*	(kg/m3)	1025	1025	*averaged*
Thermal conductivity *	(W/m*k)	0,6	0,6	*averaged*
Viscosity*	(kg/m-s) / (N*s /m2)	0,00087	0,00087	*averaged*
Prandtl		5,78985	5,78985	

Gas flow - hot		Cooler 1	Cooler 2	
Medium		**Helium**	**Helium**	
Cp	Cp (j/k*kg)	5190	5190	
M_flow	kg/s	4,074	4,074	
T_hot_1	Celsius	125	91,6	
T_hot_2	Celsius	40	40	chosen T inlet compressor
C_hot	W/K	21144,06	21144,06	
Pressure	bar	35	49	*averaged*
Density	(kg/m3)	5,4	7,6	*averaged*
Thermal conductivity	(W/m*k)	0,153	0,153	*averaged*
Viscosity	(kg/m-s) / (N*s /m2)	0,00002067	0,00002067	*averaged*
Prandtl		0,701	0,701	

LMTD - Simple		Pre-cooler	Intercooler	
Required heat transfer	Q (W)	1797245,10	1093147,90	
LMTD	K	34,49	24,73	
C_min	W/K	21144,06	21144,06	
C_Max	W/K	99825,00	99825,00	
C_ratio	-	0,21	0,21	
Material shell & Tube	-	SS316	SS316	assumption
Thermal conductivity	W/m*k	16,00	16,00	
Density_material	kg/m3	8000,00	8000,00	
Cp	J/kg*k	600,00	600,00	

Modelling Heat Exchanger Cooling (G-TL) - Shell and tube

Start dimensions		Pre-cooler	Intercooler	
Tube_D_inner	m	0,0144	0,0144	assumption
Tube_D_outer	m	0,0191	0,0191	
Tube_thickness	m	0,0023	0,0023	assumption
Pitch_factor	-	1,2500	1,2500	assumption
Pitch	m	0,0238	0,0238	
CS_1_tube	m2	0,0002	0,0002	
CS_shell_around1tube	m2	0,0003	0,0003	
CF_1_tube_outer	m	0,0598	0,0598	
A_1_tube	m2	0,1357	0,1357	G
D_hydraulic_tubes	m	0,0144	0,0144	
D_hydraulic_shell	m	0,0188	0,0188	
Tube length	m	3	3	assumption

First iteration				
U_initial_estimate	W/(m^2-C)	96,00	110,00	1st iteration assumption
Q_max	W	2008686	1302474	
A_aggregate_initial estimate	m2	542,73	401,88	
E_initial_estimate	-	0,85	0,83	
Shell passes	-	2	2	Assumption
Tube passes	-	4,00	4,00	Assumption
#tubes_required	-	999,74	740,28	

Figure B.2: Part 1: Design characteristics pre-cooler and inter-cooler for a 5.5 MWth HTGR

Flow analysis				
Speed_through_tubes	m/s	4,63	4	
Speed_through_shell	m/s	0,173	0,234	
Reynolds gas flow	-	17432	23541	
Nusselt gas flow	-	49	63	
h_conv_gas	W/(m^2-C)	524	667	
Reynolds_seawater	-	3842	5189	
Nusselt_seawater	-	10	11	fully developed flow
h_conv_seawater	W/(m^2-C)	322	356	
HTC_hot	W/(m^2-C)	524	667	
HTC_cold	W/(m^2-C)	322	356	
R_hot_convection	K/W	7,03E-06	7,47E-06	
R_cold_convection	K/W	1,14E-05	1,40E-05	
R_wall_conduction	K/W	5,35E-07	7,23E-07	
R_without_fouling		1,90E-05	2,22E-05	
U_without_fouling		96,98	112,29	
UA_without_fouling				
Fouling				
Fouling factor helium gas	m^2*K/w	0,00002	0,00002	assumption
Fouling factor sea water	m^2*K/w	0,0002	0,0002	assumption
R_Fouling cold side	K/w	1,8E-07	2,5E-07	
R_Fouling hot side	K/w	1,8E-08	2,5E-08	
Final E-NTU calculation				
R_total	K/W	1,92E-05	2,24E-05	
U_total	W/(m^2-C)	96	111	
UA_total	W/K	52076	44578	
NTU_total	-	1,23	1,05	
Effectiveness 1 shell pass	-	0,66	0,61	
Effectiveness 2 shell pass	-	0,89	0,86	
Q actual	W	1,79E+06	1,11E+06	
Thermal mass				
Steel volume tubes	m^3	1,26	0,93	
Steel weight	kg	10095	7475	
Thermal mass	J/k	6056832	4484940	
Pressure loss				
Pressure loss				
Cold_pressure_loss coefficient	-	100	100	assumption
Hot_pressure_loss coefficient		50	50	assumption
d_Pressure_cold	kPa		2,7	
d_Pressure_hot	kPa		4	

Figure B.3: Part 2: Design characteristics pre-cooler and inter-cooler for a 5.5 MWth HTGR

B.3. Detailed design recuperator used in the simulations

Heat exchanger (G - G)		
Required heat transfer	Q (W)	10464784
LMTD		29,90
C_min	W/K	21175,20
Material plate		Stainless steel SS316
Thermal conductivity	W/m*k	16
Density	kg/m3	8000
Cp	J/kg*k	600
PCHE		
Channel diameter	m	0,002
Channel pitch	m	0,00254
Plate thickness	m	0,0016
Flow length	m	1,5
t_e		0,000814602
U_initial_estimate	W/m^2-C	393
A_initial estimate	m2	890,62
A_crossection_channel		1,5708E-06
Total numbers of channels	-	115479,13
Circumference_channel	m	0,005141593
PCHE_width		0,6
Channels/plate		236,22
PCHe_height		0,78
A_p_total	m2	439,98
A_c_total		445,31
A_h_total		445,31
Cold-side inlet velocity	m/s	7,55
Hot-side inlet velocity	m/s	15,51
D_hydraulic	m	0,00122
Cold-side Rey ave	-	1682,93
Hot-side Rey ave	-	1656,31
HTC_cold	W/(m^2-(	801,63
HTC_hot	W/(m^2-(	799,45
R_cold	K/W	2,80133E-06
R_hot	K/W	2,80897E-06
R_wall_conduction	K/W	1,15717E-07
HTC_overall	W/(m^2-(	392,2743499
UA		174641,40
Required_A_Totaal	m2	892,27
NTU	-	8,25
Effectiveness	%	89%
Q_actual		9,33E+06
d_Pressure_cold	kPa	
d_Pressure_hot	kPa	
Fouling factor assumed	m^2*K/w	1,00E-04
Fouling cold side	K/w	2,25E-07
Fouling hot side	K/w	2,25E-07
R_total_incl_foul	K/W	6,18E-06
HTC_overal_inclfouli		392,21

Thermal mass		Stainless steel SS316	Alloy 800H/HT	Titanium
Weight plates	kg	2867,23874	2845,734449	1614,97222
Thermal mass	J/k	1720343,244	1565153,947	1049731,943

MATLAB

Counter flow		
Gas 1 - cold side recuperator		
min_free_flow_area	m2	0,090697098
D_h_cold	m	0,0012
Gas volume	m3	0,136045646
Length flow path	m	1,5
Heat transfer surface area	m2	445,31
Fouling factor	m^2*K/w	0,000100
Gas 2 - Hot side recuperator		
min_free_flow_area	m2	0,090697098
D_h_cold	m	0,0012
Gas volume	m3	0,136045646
Length flow path	m	1,5
Heat transfer surface area	m2	445,31
Fouling factor	m^2*K/w	0,000100

Figure B.4: Detailed design of the PCHE designed for a 10 MW recuperator for the Holos-Quad design

C

The 22 MWth Holos-Quad HTGR concept design

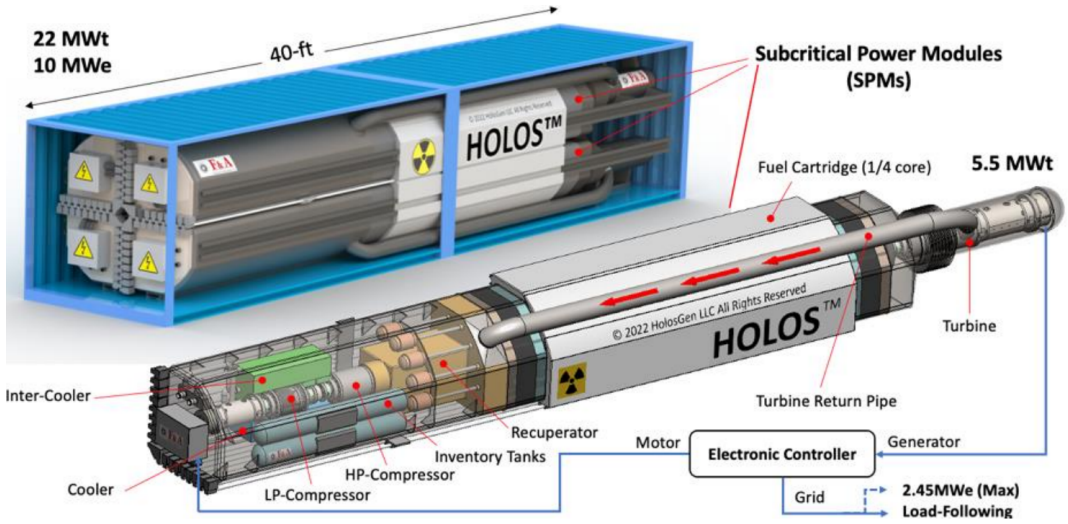

Figure C.1: Holos-Quad - A 10 MWe closed-cycle helium-cooled HTR concept in a 40-ft container. The parameters of this modular HTGR, served as a base case for the parameters chosen in the simulations within this research.

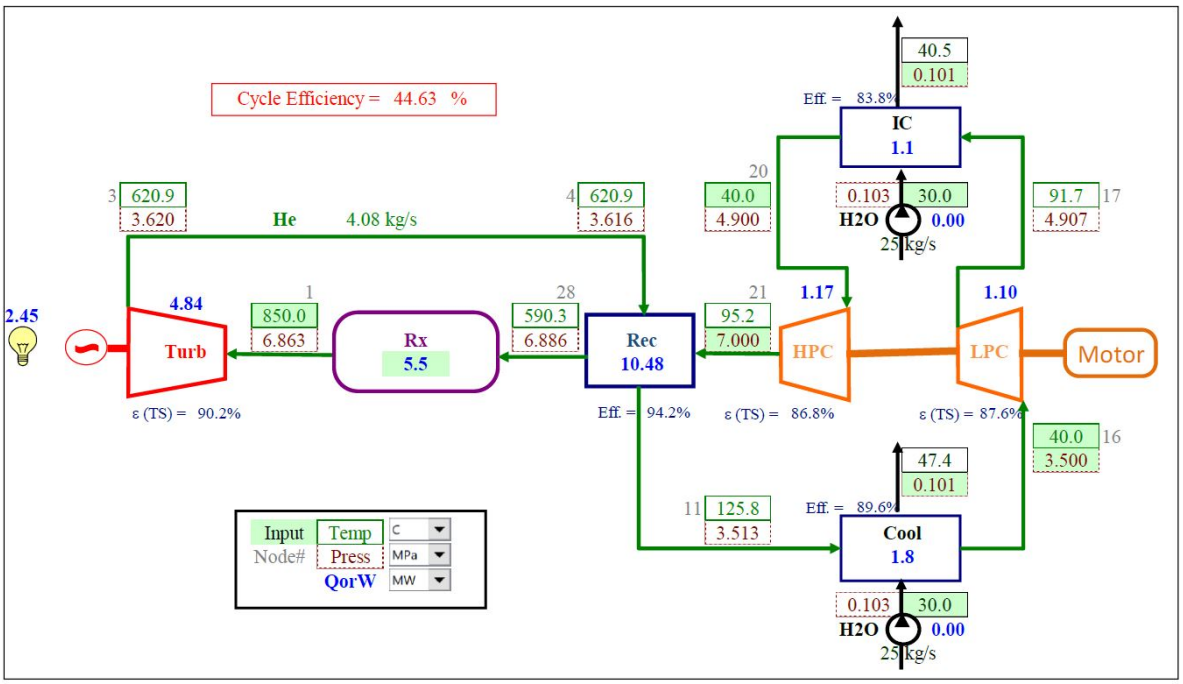

Figure C.2: Holos-Quad design conditions for 1 (out of 4) subcritical Power Modules (SPMs). This power cycle served as a base case in the thermodynamic model built for this study.

D

Other concepts

Level	Definition
TRL 9	Actual system proven
TRL 8	Actual system completed and qualified through test and demonstration
TRL 7	System/subsystem model or prototype demonstration in the planned environment
TRL 6	System/subsystem model or prototype demonstration in relevant environment
TRL 5	Component and/or breadboard validation in relevant environment
TRL 4	Component and/or breadboard validation in “laboratory” environment
TRL 3	Analytical and experimental critical function and/or characteristic proof of concept
TRL 2	Technology concept and/or application formulated
TRL 1	Basic principles observed and reported

Figure D.1: TRL scale in technology maturity level assessment [35]